Investigation of Me-TDDGA as Extractant for Grouped Actinides Separation from Lanthanides

Master thesis

Nuclear Applications - Department of Chemistry and Biotechnology

University of Applied Sciences Aachen (FH-Aachen) - Jülich Campus

In cooperation with

Forschungszentrum Jülich GmbH

Institute of Fusion Energy and Nuclear Waste Management (IFN)

Nukleare Entsorgung (IFN-2)

submitted by

Zineb Benhajjam (3542383)

Supervisors

Prof. Dr. rer. nat. Hummel Helga

Dr. Wilden Andreas

29/04/2025 – Jülich

Declaration

I hereby declare that this thesis is my own work. All sources and aids used have been properly cited and referenced. I have not used any sources and aids other than those specified.

Date	Signature

Acknowledgments

I would like to express my deepest appreciation to everyone who supported me throughout this project—whether through guidance, encouragement and kindness.

First of all, I would like to thank my supervisor, Dr. Andreas Wilden, for his constant guidance, insightful feedback and endless patience throughout this project.

I would also like to thank my supervisor Prof. Dr. Helga Hummel from the University of Applied Sciences Aachen for her role in supervising this work and for her availability during important phases of the project.

Special thanks go to Zaina Paparigas for her special guidance in the laboratory work, to Dimitri Schneider and Maximilian Henkes for carrying out the ICP-MS measurements and to Norman Lieck for his regular technical support in the laboratory.

Finally, I would like to thank my family and close friends for their unwavering support, patience and inherent belief in me - especially during the delicate periods of this work.

Abstract

The removal of minor actinides (MAs) from nuclear waste - in particular the separation of Am(III) from lanthanide (Ln) fission products - is an important step in the partitioning and transmutation (P&T) strategy aimed at reducing long-term heat load and radiotoxicity. In this study, a newly synthesized DGA ligand, 2-(2-[didecyl]-2-oxoethoxy)-*N*,*N*-didecylpropanamide (Me-TDDGA), was evaluated for its extraction performance and selectivity towards tri- and tetravalent actinides and trivalent lanthanides under different experimental conditions. While Me-TDDGA alone did not achieve significant separation between An(III) and Ln(III), the introduction of 2,6-bis(5,6-di(sulfophenyl)-1,2,4-triazin-3-yl)pyridine (SO_3-Ph-BTP) as a co-extractant showed remarkable improvements in separation factors. Additionally, the use of 2,6-bis[1-(propan-1-ol)-1,2,3-triazol-4-yl)]pyridine (PTD), a better alternative to SO_3-Ph-BTP as it obeys the CHON principle, was investigated, and higher concentrations can further improve selectivity. These results highlight the potential of multi-component extraction systems and set the stage for future optimization towards more efficient actinide-lanthanide separations.

Zusammenfassung

Die Entfernung von Minoren Actiniden (MA) aus nuklearen Abfällen - insbesondere die Abtrennung von Am(III) von Lanthanid (Ln) Spaltprodukten - ist ein wichtiger Schritt in der Partitionierungs- und Transmutationsstrategie (P&T), die darauf abzielt, die langfristige Radiotoxizität zu reduzieren. In dieser Studie wurde ein neu synthetisierter DGA-Ligand, 2-(2-[didecyl]-2-oxoethoxy)-*N*,*N*-didecylpropanamid (Me-TDDGA), auf seine Extraktionsleistung und Selektivität gegenüber Actiniden und Lanthaniden unter verschiedenen Versuchsbedingungen untersucht. Während Me-TDDGA allein keine signifikante Trennung zwischen An(III) und Ln(III) erreichte, zeigte die Einführung von 2,6-bis(5,6-di(sulfophenyl)-1,2,4-triazin-3-yl)pyridin (SO_3-Ph-BTP) als Co-Extraktionsmittel bemerkenswerte Verbesserungen der Trennfaktoren. Darüber hinaus wurde die Verwendung von 2,6-bis[1-(propan-1-ol)-1,2,3-triazol-4-yl)]pyridin (PTD) untersucht, einer besseren Alternative zu SO_3-Ph-BTP, da es dem CHON-Prinzip genügt, und höhere Konzentrationen können die Selektivität weiter verbessern. Diese Ergebnisse unterstreichen das Potenzial von Mehrkomponentenextraktionssystemen und bilden die Grundlage für künftige Optimierungen im Hinblick auf eine effizientere Trennung von Actiniden und Lanthaniden.

Table of Contents

List of Abbreviations

An(III)	Trivalent actinides
Aq.	Aqueous
BTBP	6,6‘-Bis(5,6-dialkyl)-[1,2,4]triazin-3-yl)-[2,2´]bipyridin
BTBPh	bis-triazinyl-phenanthroline
CAC	Critical aqueous concentration
CHON	Carbon, Hydrogen, Oxygen, Nitrogen
COEX	CO-EXtraction
CO_2	Carbon dioxide
$CyMe_4BTBP$	6,6‘-Bis-(5,5,8,8-tetramethyl-5,6,7,8-tetrahydro-benzo-1,2,4-triazin-3-yl)-2,2’-bipyridin
D	distribution ratio
DF	Decontamination factor
DGA	Diglycolamide
DHOA	N,N-dihexyl octanamide
DIAMEX	Diamide Extraction
DMDOHEMA	N,N′-Dimethyl-N,N′-dioctyl-2-(2-hexyloxy-ethyl)malonamid
DTPA	diethylenetriaminepentaacetic acid
EXAFS	Extended X-ray Absorption Fine Structure
EXAm	Extraction of Americium
GANEX	Grouped Actinide Extraction
HREE	Heavy Rare Earth Element
HSAB	Hard & Soft Acid Base
HDEHP	di(2-ethylhexyl) phosphoric acid
HLW	High Level Waste
HNO_3	Nitric Acid
ICP-MS	Inductively Coupled Plasma Mass Spectrometry
LREE	Light Rare Earth Element
Ln(III)	Trivalent lanthanides
LOC	Limited organic concentration
M	Metal
MA	Minor actinides

MD	Molecular Dynamics
Me-TDDGA	2-(2-[Didecyl]-2-oxoethoxy)-N,N-didodecylpropanamide
MREE	Middle Rare Earth Element
MOX	Mixed oxide fuel
NOPC	Neutral Organophosphorus Compound
Org.	Organic
P&T	partitioning and transmutation
PUREX	Plutonium Uranium Reduction Extraction
PTD	2,6-bis[1-(propan-1-ol)-1,2,3-triazol-4-yl)]pyridine
rpm	Revolution per minute
SANEX	Selective Actinide Extraction
SF	Separation Factor/ Spent Fuel
SO_3-Ph-BTP	2,6-bis(5,6-di(sulfophenyl)-1,2,4-triazin-3-yl)pyridine
TALSPEAK	Trivalent Actinide Lanthanide Separation using Phosphorus Extractants and Aqueous Komplexants
TBP	Tributyl phosphate
TDDGA	N,N, N‘,N‘-tetradecyl diglycolamide
TDdDGA	N,N, N‘,N‘-tetradodecyl diglycolamide
TEDGA	N,N,N‘,N‘-Tetra-n-ethyldiglycolamid
TODGA	N,N, N‘,N‘-tetraoctyl diglycolamide
TPH	Hydrogenated Tetrapropene
TRU	Transuranium elements
TRUEX	TRansUranic EXtraction
T3P®	Propylphosphonic anhydride

1 Introduction

Energy is fundamental to economic and social development. However, today's energy systems face several major challenges that must be urgently confronted. From regional disparities in access to energy sources to the energy-related emissions that need to be reduced as quickly as possible, not to mention the security of an uninterrupted energy supply and the burden of climate change.[1] Nowadays, nuclear power is an increasingly cost-effective source of low-carbon electricity and heat, preventing more than a billion tonnes of carbon dioxide (CO_2) emissions a year, while promoting energy system reliability, long-term security and resilience to climate change.[2] For the safe and effective utilization of nuclear energy, better technologies for recycling and disposal of radioactive waste are necessary. In particular, the management of the high-level radioactive waste (HLW) and spent nuclear fuel (SF). Spent fuel is a highly radioactive and complicated mixture of many dozens of chemical species: nearly half of the Periodic System of the elements is represented in spent fuel. Following a typical burn-up of 40 GWd/t in a light water reactor, the SF consists mainly of ^{238}U (approx. 95%), along with a small amount of residual fissile ^{235}U (0.8%). About 3-4% of the fuel consists of fission products, most of which are short-lived, and roughly 1% consists of transuranic elements (TRUs) such as Np, Pu, Am and Cm.[3] Toxicity, and in particular radiotoxicity resulting from their radioactive nature rather than their chemical form, is a measure of the risks associated with these elements. As regards the evolution of the radiotoxic inventory of nuclear waste on a geological timescale, the potential risk of vitrified waste has been estimated to exceed 10,000 years, if only U and Pu are separated from the spent fuel. However, the elimination of minor actinides (MAs: Np, Am and Cm) followed by transmutation into shorter-lived radionuclides could reduce this period to 300-500 years [4].

Industrial reprocessing of spent nuclear fuel using the PUREX (**P**lutonium **U**ranium **R**eduction **EX**traction) [5] process seeks to separate U and Pu from fission products and minor actinides, using the unique selectivity (and stability) of an organic molecule, tributyl phosphate (TBP). In this way, reprocessed plutonium can be used to manufacture mixed oxide fuel (MOX), while reprocessed uranium can be stored as a valuable material. Since they are responsible for a large part of the long-lived heat-load and radiotoxicity of the irradiated nuclear fuel, the minor actinides (MA), mainly neptunium, americium and curium, must be removed. Given that no technology is capable of selectively transmuting the minor actinides whilst they are contained in the SF, they must first be separated from the neutron-absorbing elements. Lanthanides, which account for about one third of the fission products, are strong neutron absorbers and are present in acidic solutions mainly as trivalent cations, similar to the MAs. Therefore, the separation of trivalent lanthanides and actinides has become a challenging task when it comes to demonstrating the technical feasibility and success of partitioning and transmutation (P&T) strategies designed to reduce the burden on geological disposal [4].

Most commercial and developing processes for actinide separation from spent nuclear fuel are presently hydrometallurgical processes, particularly **solvent extraction**, as shown in (Figure 1). It involves contacting an organic solvent containing an extracting ligand with an aqueous solution of spent nuclear fuel, usually dissolved in nitric acid. An optimal extraction agent

should have a high affinity and selectivity towards the target molecules, be hydrolytically and radiologically stable, readily soluble, have fast reaction kinetics and be easy to synthesize [6].

Figure 1: Solvent extraction process explained, an organic solvent (blue) with extractant molecules (blue symbols) is mixed with an aqueous phase (yellow) containing metal ions (black symbols) to maximize contact. After phase separation, the extracted ions transfer into the organic phase [6].

Due to the chemical similarities of the trivalent actinide and lanthanide elements, it proved easier in the past to develop step-by-step processes: initially An(III) and Ln(III) co-extraction processes, which also address the problem of alpha-decontamination. In Europe, this step was referred to as the DIAMEX (**DIAM**ide **EX**traction) process. And secondly, An(III)/Ln(III) separation processes, which can only be carried out with the solutions from the first step. This second step is known as the SANEX process (**S**elective **A**cti**N**ide **EX**traction) [7].

Worldwide, significant efforts have been made to develop ligands for actinide-lanthanide separation. Various classes of molecules have been explored, including neutral organophosphorus compounds (NOPCs), malonamides, nitrogen-donor extractants, and diglycolamides—the primary focus of this work. This study aims to evaluate the extractability of a novel DGA-family ligand and to further explore the chemical behaviour of *f*-elements in solution.

1.1 Fundamentals of Actinide and Lanthanide Chemistry

In the periodic table of elements, the *f*-block elements are divided into two series: lanthanides (Ln) and actinides (An) (Figure 2). Lanthanides have their last electron filling the 4*f* subshell, while actinides have a progressively filled 5*f* subshell.

Lanthanide elements (Ln: La-Lu; 57–71) belong to the rare-earth elements (REEs) (Sc, Y, and Ln). According to IUPAC nomenclature rules, they correspond to elements (Sc), (Y), and (Ln: La-Lu). Chemists classify trivalent lanthanides (Ln^{3+}) based on their electronic structure: light lanthanides (La-Gd) lack paired 4*f* electrons, while heavy lanthanides (Dy-Lu) possess them. Geochemists use a slightly different approach, excluding Eu due to its anomalous properties and sometimes defining a middle group (Nd-Tb). In metallurgy and industry, LREEs typically include La-Nd, MREEs range from Sm-Gd or Sm-Dy, and HREEs from Dy-Lu or Ho-Lu. Yttrium, chemically similar to Dy-Ho, is grouped with HREEs, whereas scandium, due to its distinct chemical and geochemical behaviour, is classified separately [8].

Actinides are the fifteen chemical elements with atomic numbers 89 to 103, the first of which is actinium (Ac) and the last of which is lawrencium (Lr). As all actinide isotopes are radioactive and exhibit a wide range of nuclear decay properties, in particular spontaneous and induced nuclear fission, the actinide series is rather unique. For the major actinides (uranium, plutonium), isotopes $^{235\text{-}238}U$ and $^{238\text{-}242}Pu$ are the ones to be considered in nuclear fuel reprocessing. In the case of the MAs (Np, Am, Cm), it is mainly the isotopes ^{237}Np, ^{241}Am and ^{243}Am as well as ^{242}Cm and ^{244}Cm. The isotopes of Np and Am exhibit both alpha and gamma decay, whereas Cm isotopes are primarily alpha emitters with significant spontaneous fission neutron emission, making them a substantial intrinsic neutron source. In addition, their decay produces considerable heat that must be effectively dissipated [9].

Ever since their discovery, actinides have been closely associated with lanthanides due to their similar physicochemical properties. However, while the lanthanides form a relatively homogeneous group, the actinides exhibit greater variability. Actinides from curium onwards resemble lanthanides in their trivalent chemistry, whereas thorium to plutonium exhibit diverse oxidation states and distinct redox behaviour [9].

The two series are not, however, entirely comparable. An essential difference lies in the oxidation states. The oxidation states of the lanthanides in aqueous solution are relatively easy to identify. While the +III state predominates, Sm, Eu and Yb can also be present in the +II state, while Ce, Pr and Tb can have a +IV state. The situation is more complicated for the actinide elements, with a large number of compounds displaying formal oxidation states ranging from +II to +VII. A fundamental distinguishing feature between early actinides and lanthanides is their ability to form oxocation species known as actinyl ions (AnO_2^{n+}) in the +V and +VI oxidation states. This property is observed in U, Np, Pu and Am, while Pa can form a monooxo species under certain conditions. In contrast to the highly localized 4*f* orbitals of the lanthanides, the 5*f* orbitals of the early actinides (Pa to Am) participate more actively in binding, resulting in hybridization with the 6d, 7s and 7p orbitals. Hence more covalent interactions with ligands, making these elements chemically similar to transition metals. As the actinide contraction becomes more pronounced, an evolution towards lanthanide-like behavior

is observed, particularly beyond Am, where the predominant oxidation state becomes +III. Excluding No, which is the most stable in the +II oxidation state [9].

The ability of actinide and lanthanide cations to enter complexes varies considerably depending on their oxidation state. The most common feature is that trivalent lanthanides and actinides behave like typical “hard acids” [10, 11]. This means that their binding to almost any ligand can be described satisfactorily by an electrostatic model. Consequently, both series of trivalent cations preferentially interact with hard bases, such as fluoride or oxygen donors, rather than softer bases, such as nitrogen, sulfur or phosphorus donors. The metal ions do interact with these soft bases in organic solvents of low solvating power but, except for nitrogen donors, they do not do so in aqueous solution. In nitrogen-containing ligands, such as amino-carboxylates, the oxygen in the ligand helps remove some water from the metal ion, making it easier for the nitrogen to attach without disrupting the surrounding water molecules too much [12].

Similar to the lanthanides, which experience a “lanthanide contraction”, a gradual decrease in ionic radii with increasing atomic number can also be observed in the actinides, referred to as “actinide contraction”. In this context, a deeper understanding of the solution chemistry of actinide and lanthanide ions was the main concern of Paola D'Angelo et al. Based on a precise experimental determination of ion-water distances obtained by combining EXAFS (Extended X-ray Absorption Fine Structure) results and MD (Molecular Dynamics) structural data, the ionic radii of An(III) cations and Ln(III) cations in aqueous solution were determined for the first time. This systematic study shows a strong analogy between the Ln(III) and An(III) series in terms of hydration properties and poses a challenge for separation processes whose efficiency is based on different behaviour in different solvents and/or selective molecules [13, 14].

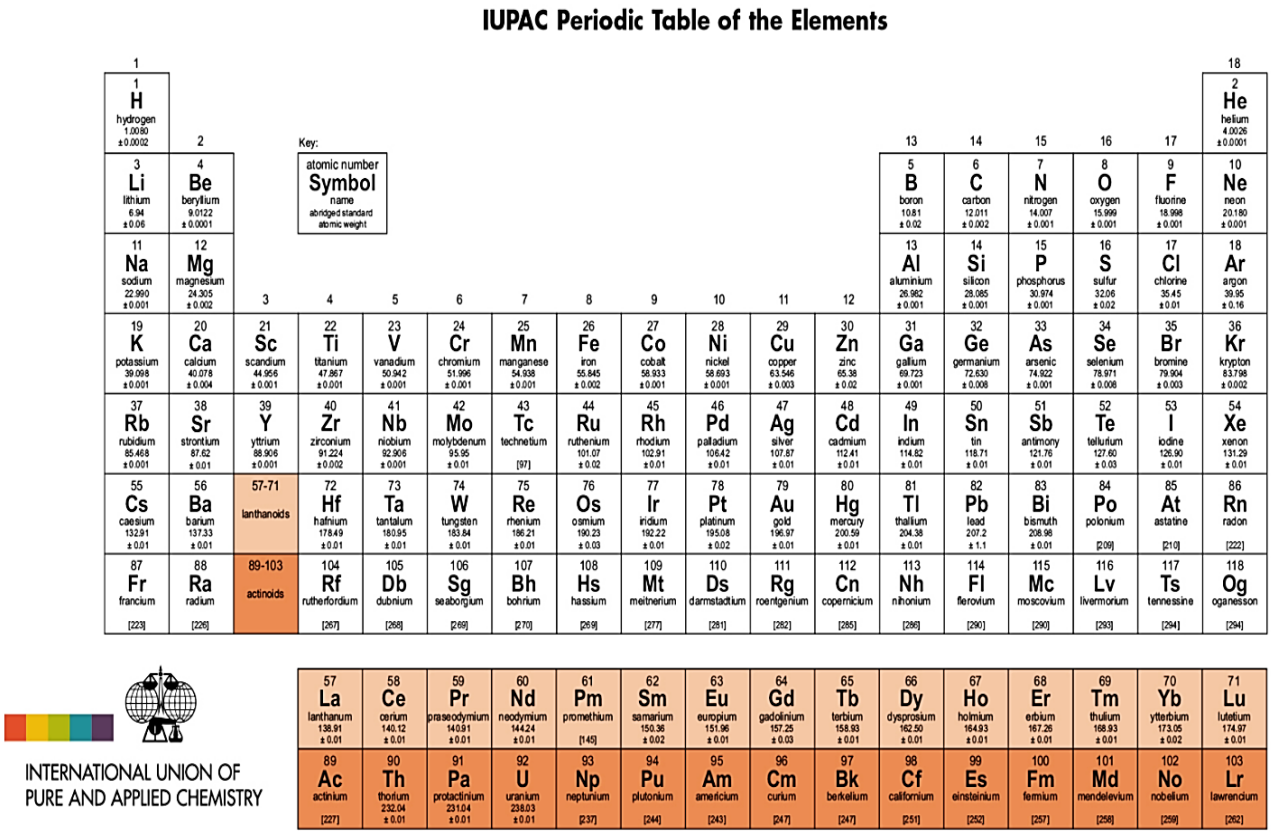

Figure 2: the IUPAC Periodic Table of the Element

1.2 Overview of Partitioning Processes

A variety of strategies have been adopted worldwide for the reprocessing of spent fuel. In Europe, the focus has been on the use of selective extractors and molecular diluents to generate a minimum amount of secondary waste. This strategy is characterized by the use of chemicals that contain only C, H, O and N atoms (often referred to as the CHON principle) [15], making them suitable for subsequent incineration. These in-depth studies have led to the development of reference aqueous separation processes, as illustrated in Figure 3 [16].

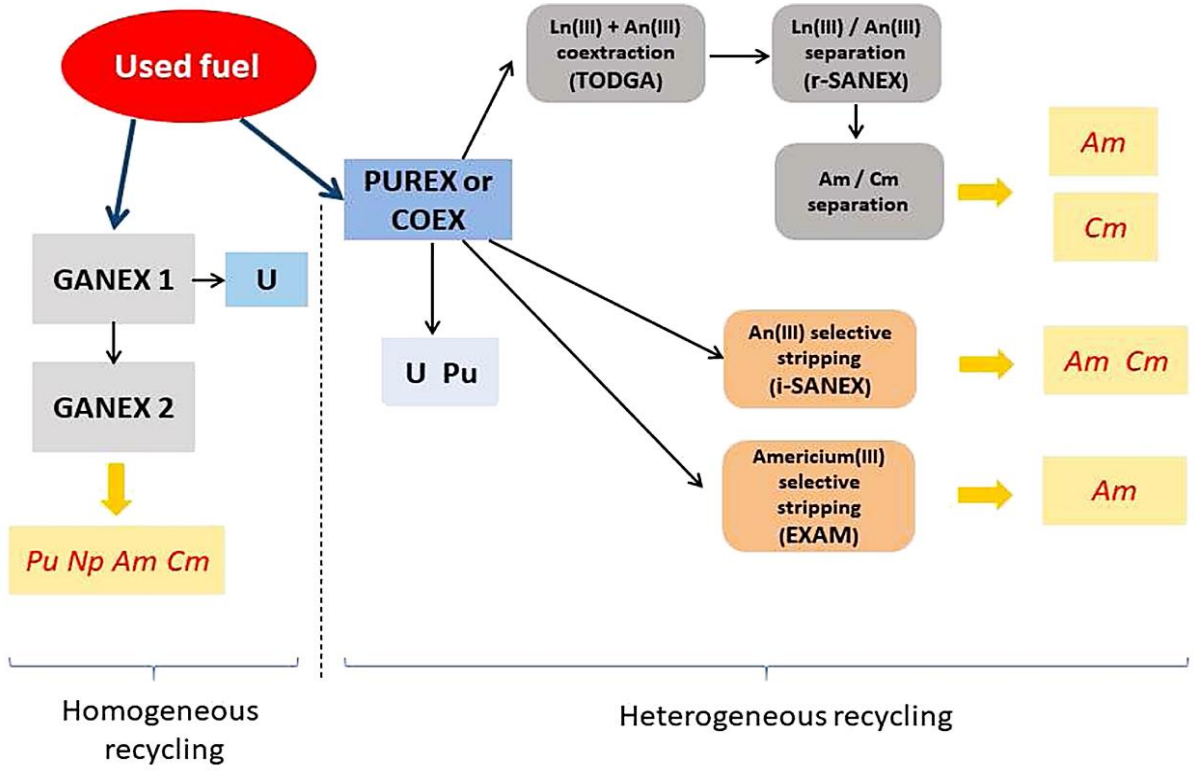

Figure 3: Europe-wide hydrometallurgical separation strategy for homogeneous and heterogeneous recycling of actinides from spent fuel [16].

Even though the PUREX process is a well-established and mature hydrometallurgical process in the nuclear industry, fundamental and application studies have continued. In fact, advanced aqueous processes are variants of the original PUREX process. The major difference between these methods lies in the nature of the separated product stream. They tend to separate either all actinides together, or all actinides except uranium together, or the minor actinides, or the fission products of interest [17].

The PUREX process is used to separate U and Pu from other fission products, using TBP as an extractant. The COEX (**CO**-**EX**traction) process is a modified version of the PUREX process, whereby it is designed to produce a U + Pu mixture (U/Pu > 20%), rather than pure plutonium. The main advantage of this process is to exclude any production of separated plutonium, in order to limit proliferation risks. It also produces a perfectly homogeneous mixed oxide for use in MOX fuel fabrication, offering enhanced performance [9].

Due to the chemical similarities of An(III) and Ln(III), separation has traditionally involved a two-step process: coextraction of An(III)+Ln(III) followed by selective An(III)/Ln(III) separation. However, modern methods now enable single-step recovery of trivalent actinides from highly active liquid waste [4].

Co-extraction of the actinides and lanthanides can be achieved by several means. The TRUEX (**TR**ans**U**ranic **EX**traction) process uses carbamoylmethylphosphine oxide (CMPO) and TBP in paraffinic hydrocarbon diluent to extract actinide and lanthanide salts from acidic feeds [6]. Developed at the CEA (Commissariat à l'énergie atomique) in France, processes known as DIAMEX, utilizing malonamide extractants such as DMDOHEMA, co-extract trivalent An and Ln from acidic feeds. These processes are directly compatible with the PUREX process and require no feed adjustments, i.e. no adjustment of nitric acid concentration between PUREX and DIAMEX solvent extraction cycles [18, 19]. The efficiency of the process has been demonstrated by trials with real HLW solutions in France and Europe. However, the process's main drawback is the partial co-extraction of the noble metals Pd and Ru along with MAs [17]. Subsequently, diglycolamide extractants were proposed to co-extract An(III) and Ln(III). Unlike malonamides, DGAs essentially feature an ether oxygen atom between the two amine groups. This electron-withdrawing oxygen atom reduces the basicity of the amide groups, making DGA extractants less acid-sensitive than malonomides. The oxygen atom also provides a third site for metal coordination, so that DGA ligands are tridentate, making them more effective extractants than bidentate malonamides [6, 18].

The first research carried out in Europe on the separation of An(III)/Ln(III) focused on the selective extraction of actinides (SANEX process) from the DIAMEX product solution (i.e., from actinides(III) and lanthanides(III) in nitric acid solutions), using extracting agents coordinating via nitrogen (BTP based processes) or sulphur donor atoms (such as Cyanex 301 process) [17].

Developed in China in 1995, the Cyanex 301 process is based on a mixture of mainly bis (2,4,4-trimethylpentyl) dithiophosphinic acid. By using 0.1 mol/L Cyanex 301 + 0.02 mol/L 2,2'-bipyridyl or 0.002 mol/L 1,10-phenanthroline in toluene as the organic phase, Am(III) and Eu(III) were extracted from 1 mol/L $NaNO_3$ + 0.02 mol/L sulfanilic acid at pH=3.2, achieving an $SF_{Am/Eu}$ of ~40,000. Although this extractant is capable of delivering excellent SF values, it is not suitable for use on realistic spent nuclear fuel solutions due to its instability to oxidizing conditions such as the presence of nitric acid [6].

A major breakthrough took place in 1999 with the development of aromatic dithiophosphinic acids and alkylated 2,6-bis(1,2,4-triazin-3-yl)-pyridines (BTPs), two families of ligands enabling the selective extraction of An(III) from acid solutions. Established in Germany, the BTP family has led to the development of advanced extractants, including bis-triazinyl-bipyridine (BTBP) [20], bis-triazinyl-phenanthroline (BTPhen) [21, 22] and CA-BTP [23], as reported in various studies.

Aromatic dithiophosphinic acids and BT(B)P molecules differ fundamentally in their chemical properties and extraction mechanisms. Whereas dithiophosphinic acids rely on sulfur donor atoms to coordinate metal ions, BT(B)P molecules use nitrogen atoms. In addition, BT(B)P

molecules obey the CHON principle, whereas dithiophosphinic acids do not fall into this category due to the presence of sulfur atoms. Their extraction behaviour also varies: BT(B)P function as neutral extractants (solvation mechanism), coextracting metal ions with their counter-anions, while dithiophosphinic acids act as acid extractants (cation exchangers), replacing protons with metal ions during extraction [3].

Building on these extractant developments, the i-SANEX (Innovative Selective Actinide Extraction) process was established as a practical application utilizing the selective coordination properties of BTPs. The i-SANEX process aims to selectively strip An(III) from the aqueous phase using SO_3-Ph-BTP in nitric acid. Results from the innovative SO_3-Ph-BTP-SANEX process show that Am(III)+Cm(III) and Ln(III) were extracted quantitatively (>99.9%) with TODGA and that very high feed/raffinate DFs were achieved with DF>10^3 [24, 25]. However, SO_3-Ph-BTP generates sulphur-containing waste streams, which should be avoided. 3,3'-(Pyridin-2,6 diylbis(1H-1,2,3-triazol-4,1-diyl))bis(propan-1-ol) (PyTri-Diol or PTD), on the other hand, is a CHON compound, allowing for its destruction to gaseous products. Wilden et at. demonstrated the i-SANEX process using PTD, where excellent DFs were achieved: The separation from Ln(III) worked very well and the corresponding An(III)/Ln(III) decontamination factors were very high DF ≥4,000 [26].

For An(III)/Ln/III) separation, the TALSPEAK (**T**rivalent **A**ctinide **L**anthanide **S**eparation using **P**hosphorus **E**xtractants and **A**queous **K**omplexants) process was developed at Oak Ridge National Laboratory in the 1960s. A phosphorus acid extractant, HDEHP, was used to recover lanthanides, while a water-soluble retaining reagent, DTPA, was used to selectively retain americium and curium in the aqueous phase. Extensive amounts of lactic acid buffer (at least 1 mol/L) were used to maintain the pH where optimal separations are obtained, pH ~ 3.5, and to accelerate the kinetics of metal phase transfer. The chemistry of organic phase aggregation in TALSPEAK was shown to exhibit abrupt pH dependencies on metal extraction, and the slow extraction kinetics were not compatible with centrifugal contactor technology. In the end, the complexity and slow kinetics of TALSPEAK chemistry and the additional processing facilities required to complete the separation of trivalent *f*-elements encouraged the adoption of other schemes [27].

During EUROPART, it was proposed to extract Am(III) and Cm(III) directly from high-level waste without prior co-extraction of An(III)-Ln(III), which could lead to a simplification of the overall An(III) recycling strategy and the elimination of the DIAMEX process. But the challenge is clear: at high nitric acid concentrations (3-4 mol/L), the extractant must have sufficient affinity for the target actinide ions, and selectivity against all fission and corrosion products present in the fuel dissolution solution [3, 18]. In single-cycle SANEX processes, a solvent containing $CyMe_4$-BTBP and TODGA in a kerosene/octanol diluent directly extracts Am(III) and Cm(III) from HLLW. Although, for example, $CyMe_4$-BTBP extracts An(III) selectively over Ln(III) from 3 to 4 mol/L HNO_3, the coextraction of Fe, Ni, Zr and Pd has hindered the development of such a process to date [3]. A promising 1-cycle-SANEX system was developed at FZJ, where the sulfur-bearing amino acid L-Cysteine showed good complexation of Pd and prevented its extraction into the organic phase without influencing the extraction of the trivalent actinides Am (III) and Cm (III) [28]. However, the sulfur content of

this solution, due to L-cysteine, can pose problems during vitrification. A further drawback is the rather slow kinetics, a common limitation of An(III)/Ln(III) separation processes using $CyMe_4$-BTBP [18].

CEA has developed the EXAm (**EX**traction of **Am**ericium) process for separating and recovering a pure americium product directly from the PUREX raffinate, which is the main contributor to the radiotoxicity and heat release inventory of conditioned HLW. This process aims to reduce these impacts and avoid the difficult recycling of Cm, due to the chemical similarities between Am(III) and Cm(III). The EXAm process is based on a mixture of HDEHP and DMDOHEMA as solvent. A water-soluble complexing agent, TEDGA, is added to the PUREX raffinate and to scrubbing section to increase the selectivity of Am/Cm and Am/heavy Ln, taking advantage of the preferential complexation of Cm and heavy Ln by this DGA. Am and light Ln (La, Ce, Pr, Nd) are thus selectively extracted by the EXAm solvent from high-nitric acid media, leaving Cm, Zr and heavy Ln (Sm, Eu, Gd) in the raffinate. Following the Mo extraction step, americium is separated from the light Ln by selective extraction using HEDTA and citric acid at pH=3, before the Ln-Fe are extracted using TEDGA and oxalic acid [3, 18].

Figure 4 summarizes the chemical structures of the key ligands mentioned above, highlighting their structural similarities.

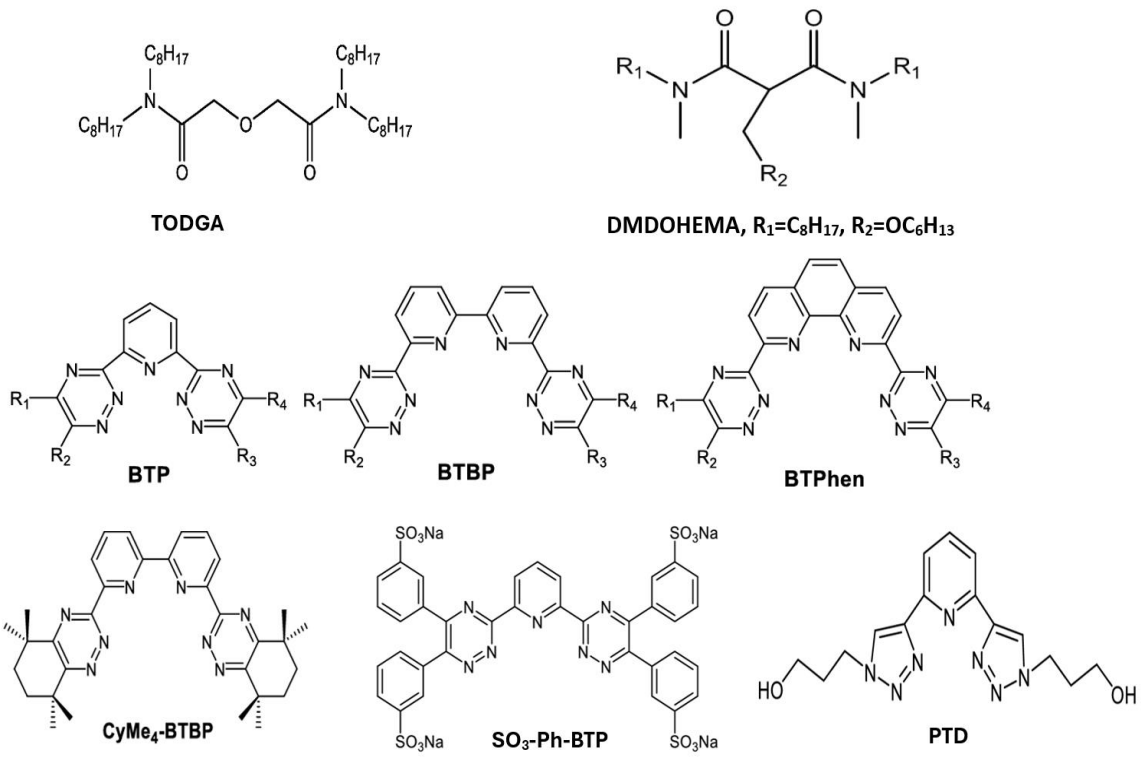

Figure 4: Chemical structure of the main ligands used in different separation processes of An and Ln.

1.3 Diglycolamides (DGAs)

Diglycolamides (DGA), which contain ether linkages between two amide groups, are well-established extractants for the coextraction of trivalent actinides and lanthanides. In terms of chemical structure (Figure 5), diglycolamides are diamides of diglycolic acid. They are used and studied as tridentate ligands with unique extraction capabilities in multiple separation processes. In line with Pearson's HSAB (Hard & Soft Acid Base) concept [11], it was postulated that nitrogen atoms were not involved in complexation and that interaction with metal ions was preferentially via hard donor oxygen atoms [29, 30].

A key factor in the extraction of metal ions is the nature of the N-substituents (alkyl chain length or branching) in DGA compounds, as this affects their hydrophilicity and lipophilicity [4, 31]. In this context, Sasaki et al. [32] reported the synthesis of a series of diglycolamides with a range of alkyl chains (from *n*-propyl to *n*-dodecyl) attached to the amidic nitrogen atoms. It was found that DGA derivatives with shorter alkyl chains (propyl and butyl) were soluble in water and therefore could be used as masking agents for *f*-block metal ions. Longer alkyl chains were virtually insoluble in water and freely soluble in paraffinic solvents and could therefore be used for actinide extraction. Distribution ratios for Am(III) with DGA extractants were found to decrease with increasing chain length due to steric hindrance induced by bulky alkyl groups during metal ion complexation [33, 34].

The most commonly used and studied DGA ligand is TODGA, due to its high solubility in *n*-dodecane and its high affinity for An(III) and Ln(III) simultaneously [35]. However, the main drawback of TODGA is that it tends to form a third phase (i.e. the organic phase breaks down into two layers, the heavier, metal-solvate-rich layer, and the lighter, diluent-rich layer, when metal charges exceed a certain level) as the metal charge increases. Tachimori et al. clarified the characteristics of third-phase formation in the TODGA-*n*-dodecane-Nd(III) extraction system and achieved satisfactory high metal loading by using DHOA as a phase modifier [36]. Modolo et al. also reported a 35% higher Nd loading of the TODGA+TBP in TPH system [37].

A thorough review of diglycolamide chemistry, including synthetic routes, has been published by Ansari et al. [29]. Diglycolamide synthesis involves a three-step procedure: formation of an anhydride in the first step, subsequent amidation of a carboxyl group with a secondary amine in the second step, and the third step in which a second carboxyl group is activated to an anhydride or chloride and the second amide bond is formed with the secondary amine. Recently, Fialová et al. proposed a synthetic route assisted by a coupling agent, propylphosphonic anhydride, commercially known as T3P®. The introduction of this agent makes it possible to carry out the synthesis in a single step, making the procedure cost-effective. [30].

Sasaki et al. tested the loading capacity of different molecules similar to TODGA using Nd. The most interesting molecules are TDDGA (with decyl side chains) and TDdDGA (with dodecyl side chains) [38, 39]. Clearly, longer side chains increase the loading capacity of the molecule. At the same time, the viscosity of the organic solvent increases with chain length, which can lead to poor fluid dynamics, particularly when metal loading is high. This may, in turn, lead to problems such as unsatisfactory phase separation or even malfunctioning solvent

extraction contactors. For future modifications, TDDGA is more advantageous as it has been shown to have a significantly higher loading capacity, around four times higher than TODGA, and has a lower viscosity than TDdDGA. Thus, R. Malmbeck et al. [39] introduced mTDDGA (Figure 5), a double methylated TDDGA, as a candidate for the GANEX process in order to replace solvent mixture TODGA and DMDOHEMA [39]. Verlinden et al. [40] conducted solvent optimization studies of mTDDGA, with regards to the extraction characteristics of the different diastereomers of mTDGA and of mixed diastereomer solutions. In addition, radiolytic stability of mTDDGA as well as its degradation products were determined and quantified. Reported extraction results suggest encouraging prospects for the development of a new EURO-GANEX process using a mTDDGA solvent.

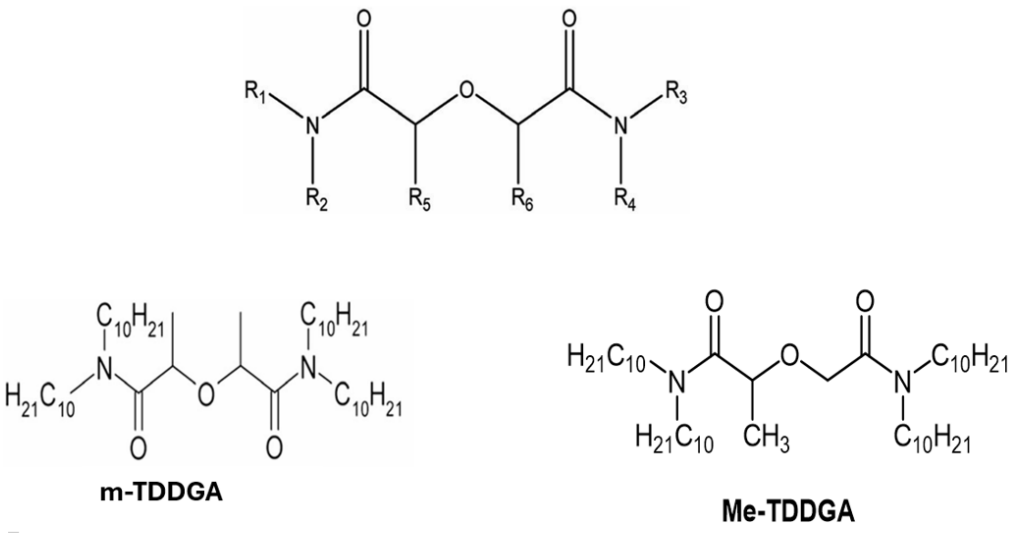

Figure 5: Chemical backbone of diglycolamides, Positions R_1-R_6= alkyl or H, along with promising modified diglycolamides for grouped actinide separation: m-TDDGA and Me-TDDGA. [40]

2 Scope of the work

The aim of this work is to study the extraction properties of a new DGA extractant, Me-TDDGA (Figure 5), its affinity for trivalent lanthanides and actinides, and to get an idea of the stoichiometry based on the Ln(III) and An(III) formed. Doubly methylated mTDDGA, previously studied by Verlinden et al. [40], can take the form of two different diastereomers, the (*R*,*S*) configuration and the (*S*,*S*) or (*R*,*R*) configuration, depending on the orientation of the methyl groups. This apparently insignificant detail has a considerable influence on the complexation capacities of the extractants. Indeed, remarkable fluctuations in extraction of up to two orders of magnitude between the two diastereomers have been reported [40]. Me-TDDGA, on the other hand, has the advantage of exhibiting no diastereomers, having a single methyl group (less steric hindrance) and respecting the CHON principle.

By adjusting key chemical factors, it is possible to separate trivalent An(III), mainly MA, from Ln(III). Thus, in this work, numerous parameters were modified to better understand the extraction behavior of Me-TDDGA. Firstly, the dependence of nitric acid and ligand concentration was studied. Then, batch extraction experiments were carried out under different T points and extraction kinetics were studied by varying the shaking time.

Me-TDDGA possesses a long side chain that enables it to cope with high metal loadings, unlike its TODGA analogue, making it a promising extraction agent. To this end, Me-TDDGA in the *n*-dodecane + HNO_3 extraction system was subjected to two loading tests: loading with Nd in the first instance, due to the chemical similarities between Nd(III) and Am(III), and then with Th(IV) in the second. This would provide a better understanding of potential Pu(IV) loading.

As DGA's hard oxygen donor atoms does not allow the trivalent metal groups 4*f* and 5*f* to be distinguished, water-soluble ligands were introduced into the aqueous phase to create a combined system: SO_3-Ph-BTP and PTD were selected for this purpose, based on the excellent results obtained by the i-SANEX or EURO-GANEX processes.

Ultimately, the results of this work should contribute to a better understanding of the extraction behaviour and chemistry of *f*-elements.

3 Experimental Methodology

3.1 Chemicals and materials

The ligand Me-TDDGA was purchased from Technocomm Ltd (Wellbrae, Scotland) and diluted in *n*-dodecane (Sigma Aldrich). SO_3-Ph-BTP and PTD were obtained from Karlsruhe Institute of Technology (KIT). Nitric acid solutions were prepared by diluting 65% nitric acid from Merck. Dilute lanthanide solutions in HNO_3 were prepared using various lanthanide chlorides and nitrates from Sigma Aldrich and Alfa Aesar. Neodymium solutions were prepared by diluting the neodymium (III) nitrate hexahydrate crystals from (Alfa Aesar) in nitric acid (Merck). All dilutions of the aqueous solutions were performed with ultrapure water (18.2 MΩcm). The radiotracers ^{241}Am, ^{244}Cm and ^{152}Eu were purchased from Oak Ridge National Laboratory (USA) and Eckert & Ziegler Nuclitec GmbH (Braunschweig). ^{239}Pu, ^{237}Np, ^{232}Th and U-nat tracers were used from laboratory stock solutions. A preparation mixture of 1% Zapon varnish (Zweihorn, Akzo Nobel Hilden GmbH) in acetone (Merck) was used for alpha spectrometry. Triton® X-100 (Carl Roth) served as a tenside for the preparation of organic ICP-MS samples.

The aqueous and organic phases were contacted on an IKA VIBRAX VXR rotary shaker. The temperature was set using a thermostat from JULABO GmbH. The samples were centrifuged with a centrifuge from Andreas Hettich GmbH. For gamma spectrometry, a HPGe (high-purity germanium) detector from Canberra was used, which was coupled with the GammaVision software for peak analysis. Alpha spectrometry was performed using an Ortec/Ametek ALPHA-ENSEMBLE-8 eight-chamber system equipped with PIPS detectors. ICP-MS (inductively coupled plasma mass spectrometry) analysis was conducted using a NexION 2000C from Perkin Elmer.

3.2 Batch Extraction Experiments

3.2.1 General procedure

The extraction system consists of 500 µL of organic phase brought into contact with 480-500 µL of aqueous phase loaded with the following radiotracers: ^{152}Eu, ^{241}Am, ^{244}Cm, ^{239}Pu, ^{237}Np and U-nat, each with a specific activity of approx. 1 kBq/mL. Extraction in 2 mL vials was carried out at a temperature of 22°C, and the samples were shaken for 30 minutes using a rotary shaker (2500 rpm). After shaking, the samples were centrifuged at 3250 rpm for 5 minutes prior to manual phase separation.

From each phase, 200 µL were taken to analyze the gamma energies of ^{241}Am (59.5 keV) and ^{152}Eu (120.8 keV) using a HPGe detector. Data acquisition and spectral analysis were performed using GammaVision software to identify the radionuclides and determine their activities.

Alpha spectrometry analysis of the actinides ^{239}Pu (5245 keV), ^{241}Am (5637 keV), ^{237}Np (4957 keV), ^{232}Th (4081 keV) and ^{244}Cm (5902 keV) was performed. Aliquots of 10 µL of each phase were mixed with 100 µl of 1 vol% Zapon varnish in acetone. The sample was then transferred

to a metal plate using a pipette, dried under a heating lamp before being fixated with gas-flame burner. Measurements were carried out for 24 hours or until 10,000 net counts were reached for reliable statistics. Concerning the quantitative analysis of non-radioactive elements by ICP-MS, aqueous samples were diluted 1:500 in 1 % HNO_3, while organic samples were prepared in the presence of 0.2 % Triton® X-100 as tenside matrix.

3.2.2 Data Analysis

To evaluate the obtained data from different analytical methods, distribution ratios (D) were calculated as the ratio of the activity or metal ion concentration (M) in the organic phase to the activity or metal ion concentration in the aqueous phase, as shown in equation (1).

$$\mathrm{D} = \frac{[M]_{org.}}{[M]_{aq.}} \qquad 1$$

The Np distribution ratios (D) were only determined in the nitric acid variation section, where measurable values were obtained. However, after reducing the amount of Np, the D values fell below the lower detection limit. Therefore, the Np data will not be considered in the next analyses and graphical representations.

The distribution ratios were plotted on a logarithmic scale against the varied parameter to interpret the experimental data. This allows the linearity of the system to be assessed. Lower and upper detection limits were defined to ensure reliable data. In this range, distribution ratios between 0.01 and 100 define a linear system with a standard deviation of less than 10%. The uncertainty increases, however, considerably outside this range due to detection limits and increased sensitivity of the system to experimental and statistical errors. Furthermore, the separation factor (SF) between two metal ions was calculated as the ratio of the corresponding distribution ratios, as shown in equation (2).

$$SF_{M_1/M_2} = \frac{D_{M_1}}{D_{M_2}} \qquad 2$$

In order to verify the stability of the extraction system (i.e. the absence of a third phase or precipitation), mass balances were also calculated as the sum of the masses or activities in the organic and aqueous phases.

To determine the stoichiometry of solvent extraction equilibrium, slope analysis of the distribution ratios as a function of the ligand concentration was carried out.

3.2.3 Influence of HNO_3

To investigate the influence of nitric acid on the extraction behaviour of lanthanides and actinides, aqueous phases containing lanthanide metal ions of 10^{-5} mol/L (Ln-all solution) in different nitric acid concentrations ranging from 0.052 mol/L to 3.80 mol/L were used. The organic phase consisted of 0.20 mol/L Me-TDDGA diluted in *n*-dodecane.

3.2.4 Influence of Me-TDDGA Concentration

The effect of the ligand concentration on the separation of actinides from lanthanides was investigated as follows: 1.074 mol/L of nitric acid with 10^{-5} mol/L lanthanide metal ions served as aqueous phases, whereas organic phases consisted of different concentrations of Me-TTDGA in *n*-dodecane, ranging from 0.04 to 0.40 mol/L.

3.2.5 Extraction Kinetics

The aim of these experiment series was to determine the time required for the system to attain equilibrium. Aqueous phases consisted of 1.074 mol/L of nitric acid with 10^{-5} mol/L lanthanide metal ions and were brought into contact with organic phases containing 0.20 mol/L of Me-TDDGA diluted in *n*-dodecane. Samples were shaken for 1, 5, 10, 15, 30 and 60 min.

3.2.6 Temperature Dependence of Extraction

The effect of temperature on the extraction behaviour of actinides and lanthanides was studied as follows: aqueous phases consisted of 1.074 mol/L of nitric acid with 10^{-5} mol/L lanthanide metal ions, and organic phases consisted of 0.20 mol/L of Me-TDDGA diluted in n-dodecane. The two phases were shaken for 30 minutes at 5, 15, 25, 35, 45 and 60 °C.

3.3 Organic Phase Loading

3.3.1 Nd-Loading

For the purposes of this experiment, neodymium was used as a representative of the trivalent lanthanides. Various Nd(III) solutions ranging from 0.01 to 0.10 mol/L in 2.236 mol/L nitric acid served as aqueous phases and were contacted with organic phases consisting of 0.2 mol/L of Me-TDDGA diluted in *n*-dodecane. Samples were shaken for 30 min at a constant temperature of T = 22°C. Then, the two phases were separated by centrifugation at 3250 rpm for 10 minutes. The concentrations of Nd(III) in aqueous phases, determined by ICP-MS, as well as D_{Nd} were plotted against the initial concentration of Nd(III) in the aqueous phase.

3.3.2 Th-Loading

Thorium was used as a representative of the tetravalent actinides to test the loading of Me-TDDGA with increasing concentrations of Th(IV) solutions, stepwise from 0.01 to 0.06 mol/L. As organic phase, 0.2 mol/L Me-TDDGA in *n*-dodecane was used. Samples were shaken for 30 min at a constant temperature of T = 22°C. Then, the two phases were separated by centrifugation at 3250 rpm for 10 minutes. The concentrations of Th(IV) in organic phases, determined by ICP-MS, and D_{Th} were plotted against the initial concentration of Th(IV) in the aqueous phase. Aliquots of 10 µL of each phase were mixed with 100 µl of 1 vol% Zapon varnish in acetone to perform alpha spectroscopy.

3.4 Combined Extraction Systems

3.4.1 Me-TDDGA and SO_3-Ph-BTP

The aim of this extraction series is to investigate the influence of the co-extractant, SO_3-Ph-BTP, on the extraction capability of Me-TDDGA. For this purpose, 0.02 mol/L of SO_3-Ph-BTP

was dissolved in 0.052 to 3.80 mol/L HNO_3 with 10^{-5} mol/L of the lanthanides. As organic phases, 0.20 mol/L of Me-TDDGA diluted in *n*-dodecane was used. After shaking, the samples were centrifuged at 3250 rpm for 5 minutes prior to manual phase separation. The analysis of samples was again carried out as described in section 3.2.1 above.

3.4.2 Me-TDDGA and PTD

Similar to the combined system described above, the extractability of Me-TDDGA is investigated in the presence of another water-soluble co-extractant, PTD. The aqueous phase consists of 0.02 mol/L PTD dissolved in 0.052 to 3.80 mol/L HNO_3 with 10^{-5} mol/L of the lanthanides. Concerning the organic phases, 0.20 mol/L Me-TDDGA diluted in n-dodecane was used. After shaking, the samples were centrifuged at 3250 rpm for 5 minutes prior to manual phase separation. The analysis of samples was again carried out as described in section 3.2.1.

4 Results and Discussion

The first section of this chapter deals with data obtained by varying different factors and their influence on the extraction process. The focus was on the following key parameters: nitric acid concentration, ligand concentration and temperature variation. To better visualize the extraction trends, the distribution ratio was plotted on a logarithmic scale as a function of the varied parameters. In the second part, the kinetics of metal transfer between the aqueous and organic phases was investigated to gain insight into the extraction mechanism. The time required to reach equilibrium was determined by plotting the distribution ratio (D) as a function of time. In the third section, the results of loading tests are presented to provide information on the loading capacity of neodymium and thorium. The formation of the third phase was visually and analytically investigated. The last section was dedicated to the impact of water-soluble soft-donor ligands, SO_3-Ph BTB and PTD, on the extraction behaviour in combination with Me-TDDGA.

4.1 Extraction behaviour

The efficiency of An(III) and Ln(III) extraction by Me-TDDGA is significantly influenced by the nitric acid concentration, the ligand concentration, the temperature and the extraction equilibria. Extraction experiments were performed with different nitric acid concentrations up to 3.38 mol/L to determine their influence on the extraction mechanism. The effect of ligand concentration on extraction was investigated by varying the ligand concentration from 0.04 to 0.4 mol/L at 1.074 mol/L; a slope analysis was performed to determine the metal-to-ligand ratio. The influence of temperature on the extraction behaviour was investigated in a range from 5 to 60°C. In addition, the kinetics were tested by varying the mixing time in batch experiments at 1.074 mol/L HNO_3. The following results illustrate the influence of these parameters on the distribution ratio of An(III) and Ln(III), the efficiency of the extraction process and allow the identification of extraction trends.

4.1.1 Influence of HNO_3

Assuming that the extraction takes place following a solvation mechanism, the extraction reaction is given by equation (3):

$$M^{n+}_{(aq)} + mL_{(org)} + nNO^-_{3\,(aq)} \rightleftharpoons [M(L)_m(NO_3)_n]_{org} \qquad 3$$

With M representing the metal ion and L the ligand and m and n are stoichiometric constants.

The mass action law applied to the extraction reaction (3) results in the equilibrium constant K_{ex} given by the equation (4).

$$K_{ex} = \frac{[M(L)_m(NO_3)_n]_{org}}{[M^{n+}]_{aq}\,[L]^m_{org}\,[NO^-_3]^n_{aq}} \qquad 4$$

The dependence of the distribution ratio D of the various metal ions on the initial concentration of HNO_3 in the aqueous phase is shown in Figure 6. D increases with increasing nitric acid concentration from 0.05 to 3.38 mol/L and reaches its highest value at the highest nitric acid concentration. A simple application of Le Chatelier's principle to equation 3 could explain the observed trend. With increasing nitric acid concentration (i.e. increase in $[NO_3^-]$), the equilibrium shifts towards the complexation reaction. It is noteworthy that neptunium has significantly lower D values compared to other actinides. The ^{237}Np tracer used contains mainly Np(V), and it is known that Np speciation has an enormous influence on its extraction. Diglycolamides are known to show low extraction of formally pentavalent metal ions [40].

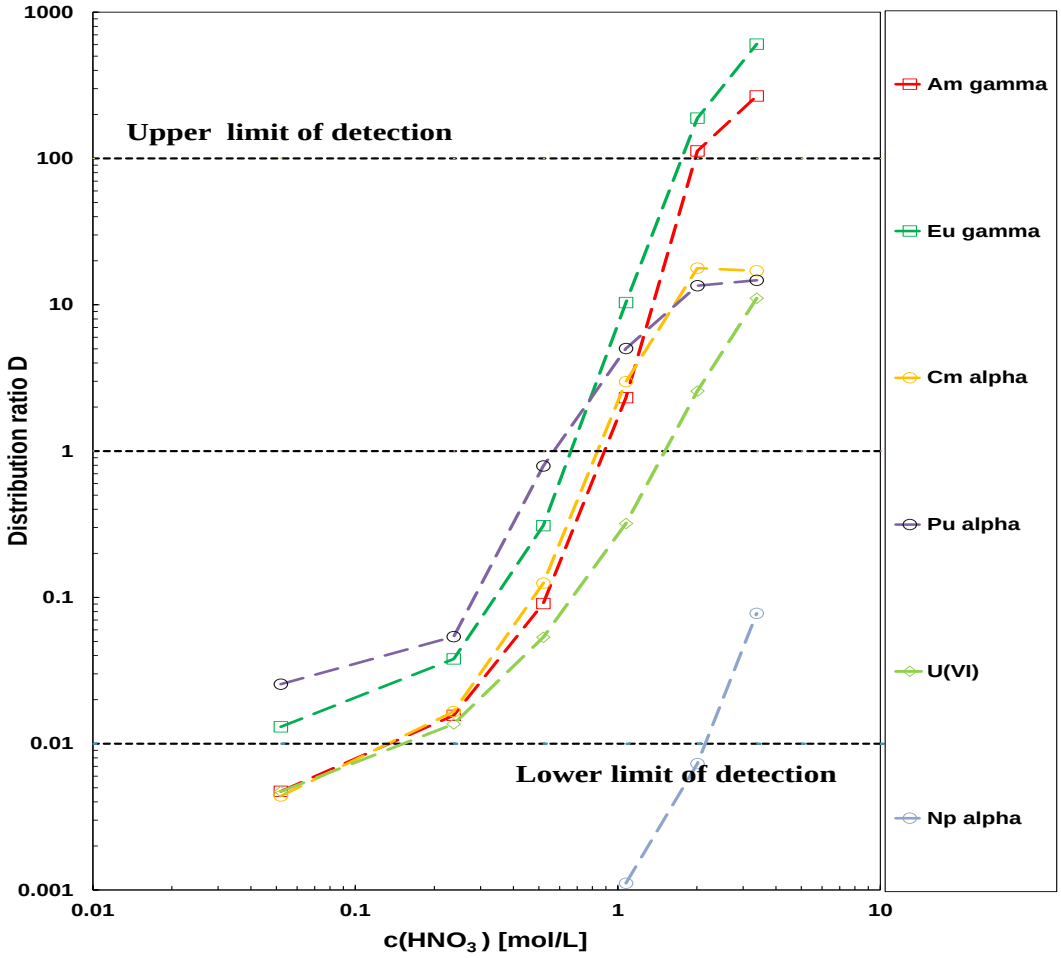

Figure 6: Distribution ratios of different radiotracers as a function of HNO_3 concentration. Organic phase: 0.2 mol/L Me-TDDGA in n-dodecane. Aqueous phase: 0.05 to 3.38 mol/L HNO_3, 10^{-5} mol l/L Ln (III) (without Pm, +Y), ^{241}Am, ^{244}Cm, ^{152}Eu, ^{239}Pu, ^{237}Np, U-nat, , t = 30 min, T = 22°C ± 1°C.

The $SF_{Cm/Am}$ values ranged from 1.00 to 1.34, indicating a minimal selectivity, which is in agreement with the chemical similarity of the trivalent actinides. At the same time, the $SF_{Eu/Am}$ values showed slightly greater variability (1.68-4.47), indicating a low selectivity for lanthanides (Eu) over Am. However, there was high variability in the $SF_{Pu/Am}$ values (0.795-7.375), possibly due to the speciation of Pu under the extraction conditions, which leads to higher complexity. In terms of uranium behaviour, $SF_{Am/U}$ between 0.8 and 1.7 were observed, indicating limited selectivity of Am over U under these conditions. High SF values, almost 50,

were obtained with higher nitric acid. Although this introduces uncertainty, it may also reflect a genuine preference for Am(III), which forms stronger complexes with the extractant compared to U(VI). It is also noteworthy that the separation factors for all metal ions did not increase with increasing nitric acid concentration, but showed strong fluctuations and no clear trend.

The extraction of the lanthanide series (w/o Pm +Y) was studied using solutions of all Ln(III) in different nitric acid concentrations (0.05–3.38 mol/L HNO_3), as shown in Figure 7. The same trend was observed as for the actinides; the distribution ratios increase with increasing nitric acid concentration. Another striking trend appears for lanthanides, which has already been studied by Sasaki et al. [32]: The distribution ratio increases with increasing atomic number, suggesting a strong correlation between the ionic radius and the distribution ratio.

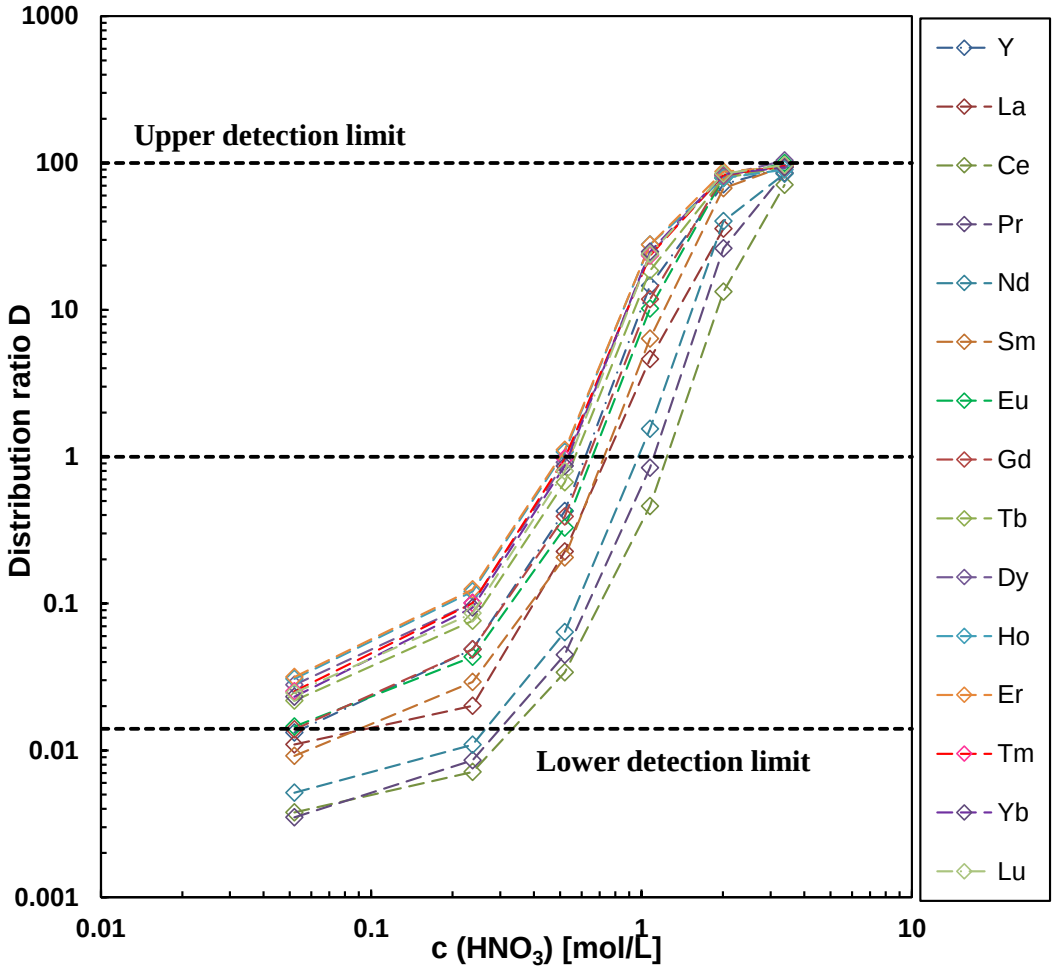

Figure 7: Distribution ratios of lanthanides as a function of HNO_3 concentration. Organic phase: 0.2 mol/L Me-TDDGA in n-dodecane. Aqueous phase: 0.05 to 3.38 mol/L HNO_3, 10^{-5} mol l/L Ln (III) (without Pm, +Y), ^{241}Am, ^{244}Cm, ^{152}Eu, ^{239}Pu, ^{237}Np, U-nat, , t = 30 min, T = 22°C ± 1°C.

For a better visualization of this trend, Figure 8 illustrates distribution ratios of Ln(III) and An(III) (Am(III) and Cm(III)) as a function of the inverse ionic radius at 1.074 mol/L HNO_3. The values for the ionic radii of the trivalent lanthanides and actinides are taken from the publications by Paola D'Angelo et al. [13, 14]. As the ionic radius decreases with increasing atomic number due to lanthanide contraction, the distribution ratio increases. However, a

maximum is reached for Er(III) with this ligand, after which the distribution ratios decrease slightly. Wilden et al. [41] observed the same trend with Me-TODGA as ligand. This is attributed to steric hindrances caused by methylation near the central oxygen donor atom. As a result of lanthanide contraction, the ligands in the complex are crowded closer together, which increases steric repulsion and leads to lower distribution ratios [41]. In addition, the low selectivity of Me-TDDGA for Am(III) and Cm(III) is, graphically, evident. As an example, the separation factors of Eu over Am and Cm are presented, with $SF_{Eu/Am}$ approximately 4.5 and $SF_{Eu/Cm}$ around 3.5.

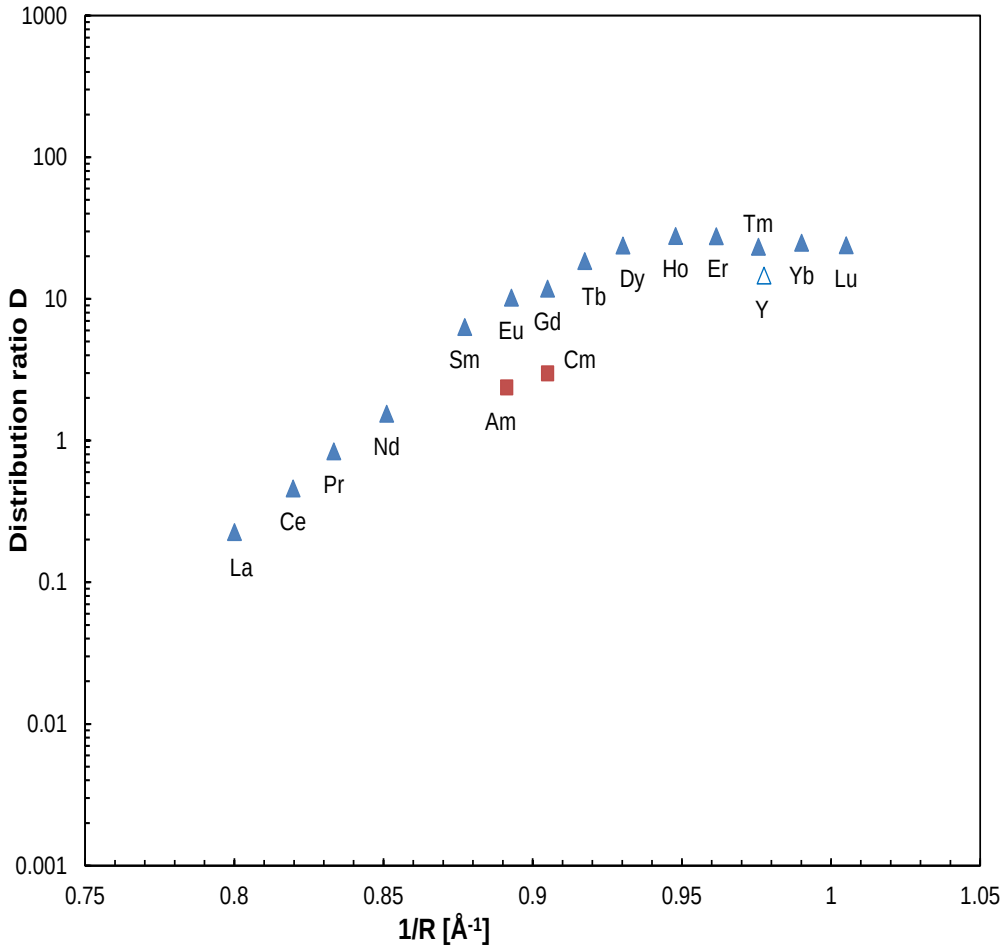

Figure 8: Distribution ratios of Ln series (w/o Pm, + Y blue), Am and Cm (orange) as function of the inverse ionic radius for extraction at 1,079 mol/L HNO_3.

4.1.2 Influence of Me-TDDGA Concentration

According to equation (3), an increase of the ligand concentration causes an increase of the distribution ratios. As shown in Figure 9, D increases for all metal ions with increasing Me-TDDGA concentration from 0.04 to 0.40 mol/L and reaches its highest value at the highest ligand concentration. However, the distribution ratios of neptunium show a discontinuity and are all below the lower detection limit. Pu(IV) and U(VI) display a bend at the ligand concentration c(Me-TDDGA) = 0.2 mol/L, showing a slight decrease in D values before increasing again. Verlinden et al. investigated the ligand dependence using double methylated TDDGA (m-TDDGA) and observed a continuous increase in the distribution ratio values for

Pu(IV) [40]. The observed kink in the distribution ratio values could therefore be due to experimental inconsistencies such as phase separation or changes in the metal ion oxidation state.

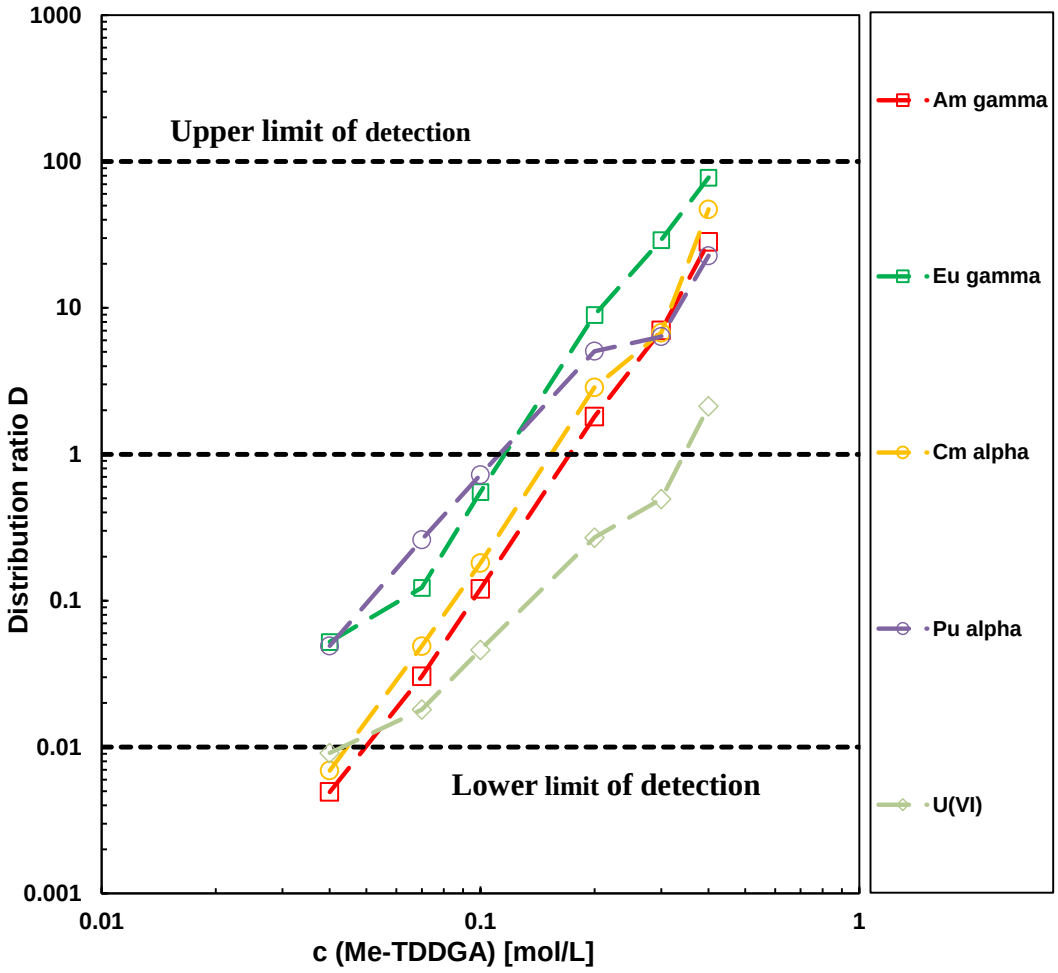

Figure 9: Distribution ratios of the various metal ions as a function of the Me-TDDGA concentration. Organic phase: from 0.04 to 0.4 mol/L Me-TDDGA in n-dodecane. Aqueous phase: 1,074 mol/L HNO_3, 10^{-5} mol/L Ln(III) (without Pm, +Y), ^{241}Am, ^{244}Cm, ^{152}Eu, ^{239}Pu, ^{237}Np, U-nat, , t = 30 min, T = 22°C ± 1°C.

As shown in Table 1, the separation factors of different metal ions with respect to Am(III) were evaluated as a function of ligand concentration at constant nitric acid concentration. The SF values show a fluctuating trend with some inconsistencies mainly due to slight experimental variations. In particular, $SF_{Eu/Am}$ and $SF_{Pu/Am}$ decrease with increasing ligand concentration, with the highest SF obtained at the lowest ligand concentration. Furthermore, $SF_{Eu/Am}$ are between 10.6 and nearly 2.8, indicating selectivity of Eu over Am, while $SF_{Pu/Am}$, which are almost all above 1, indicate better extraction of Pu over Am. However, the selectivity decreases and reverts as the values drop drastically at the last point (c(Me-TDDGA) = 0.4 mol/L). The $SF_{Cm/Am}$ values stagnate at 1.4 without increasing with increasing ligand concentration, again indicating a limited selectivity of Cm over Am. In contrast to the unclear trends observed for the other metal ions, the $SF_{Am/U}$ values show a higher selectivity of Am(III) over U(VI) as they jump from 1.7 to 14.2 at 0.2 mol/L Me-TDDGA.

Nitric acid and ligand concentrations were varied individually, maintaining a common experimental point, which is as follows: c(HNO_3) = 1.074 mol/L and c(Me-TDDGA) = 0.20 mol/L. Despite the inconsistencies observed in this section, the $SF_{M/Am}$ values at this point were comparable for almost all metal ions, except for $SF_{Am/U}$, which shows a significant deviation: $SF_{Am/U}$ = 7.3 when c(HNO_3) was varied and $SF_{Am/U}$ = 14.2 when the ligand concentration was varied.

Table 1: Separation factors $SF_{M/Am}$ (M=Eu, Cm, Pu) and $SF_{Am/U}$ for extractions with different Me-TDDGA concentrations (0.04 -0.4 mol/L) in n-dodecane and 1.074 mol/L HNO_3 including 10^{-5} mol/L Ln(III) (without Pm and Y).

	c(HNO_3) = 1.074 mol/L			
c(Me-TDDGA) [mol/L]	**$SF_{Eu/Am}$**	**$SF_{Cm/Am}$**	**$SF_{Pu/Am}$**	**$SF_{Am/U}$**
0.04	10.6	-	8.2	-
0.06	4.0	1.3	6.7	1.7
0.08	4.6	1.3	5.2	2.6
0.10	5.0	1.3	2.4	6.7
0.20	4.2	1.3	1.2	14.2
0.40	2.8	1.4	0.7	13.3

Concerning the effect of increasing the ligand concentration on lanthanide extraction, distribution ratios of the lanthanide series was plotted against Me-TDDGA concentrations in Figure 10. The distribution ratio of all elements increased proportionally with the increase in ligand concentration, before decreasing slightly at c(Me-TDDGA) = 0.2 mol/L and then increasing again at the last concentration point c(Me-TDDGA) = 0.4 mol/L. Analogous to the effect observed in section 4.1.1, the distribution ratio values increase until they reach a maximum, this time at Tm(III) instead of Er(III).

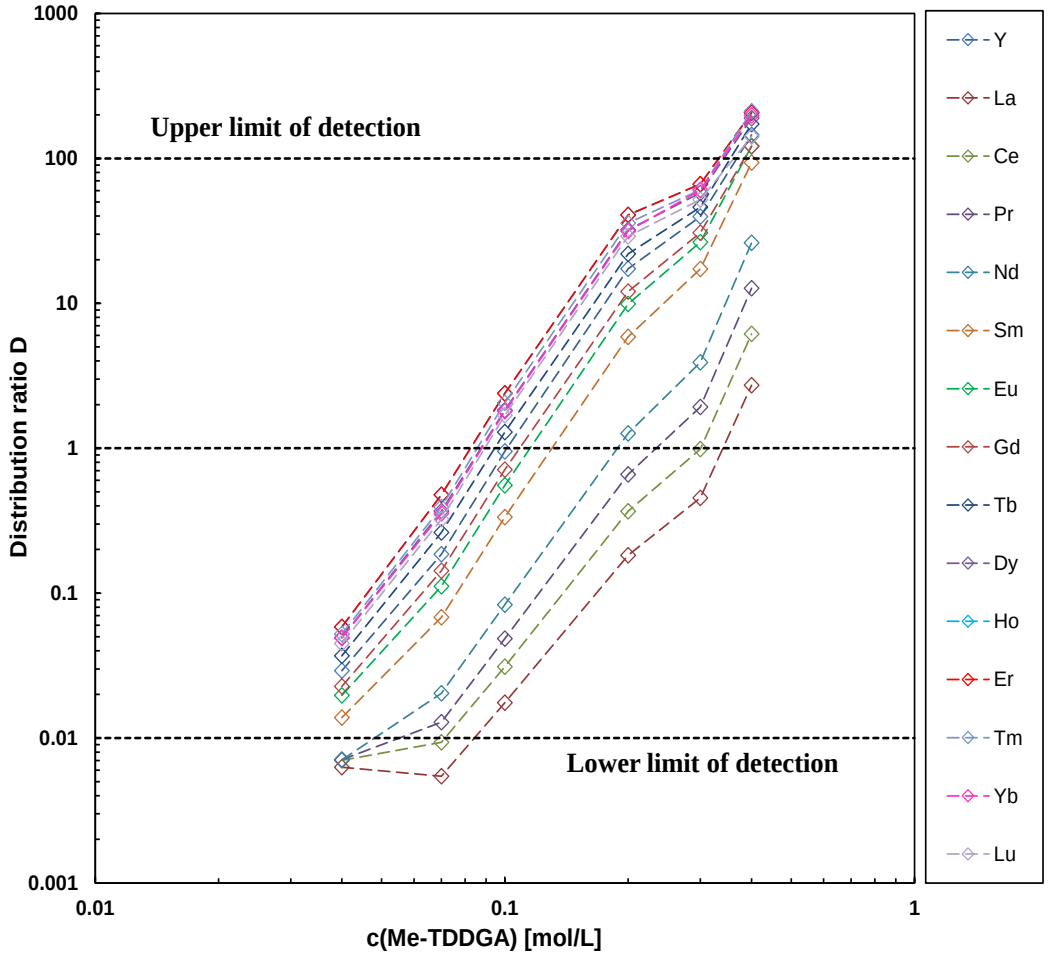

Figure 10: Distribution ratios of lanthanides against Me-TDDGA concentration. Organic phase: from 0.04 to 0.4 mol/L Me-TDDGA in n-dodecane. Aqueous phase: 1,074 mol/L HNO_3, 10^{-5} mol/L Ln(III) (without Pm, +Y), ^{241}Am, ^{244}Cm, ^{152}Eu, ^{239}Pu, ^{237}Np, U-nat, , t = 30 min, T = 22°C ± 1°C.

Furthermore, the slope of the logarithm of the distribution ratio versus the logarithm of the ligand concentration at constant nitric acid concentration provides the metal-ligand stoichiometry.

The distribution coefficient, D, can be substituted into the equation (4), which gives the following:

$$K_{ex} = \frac{D}{[L]_{org}^{m}\,[NO_3^-]_{aq}^{n}} \qquad 5$$

By taking the logarithm of equation (5), one can obtain equation (6):

$$\log(D) = \log K_{ex} + m \cdot \log([L]) + n \cdot \log([NO_3^-]) \qquad 6$$

At a constant nitric acid concentration, which is the case here, m represents the slope of the lines obtained from linear regression of the log(D) values plotted against the log([L]) concentrations.

Figure 11 shows the results of the extraction at 1.074 mol/L HNO_3 with variation of the Me-TDDGA concentration. Slopes of about three to four were observed for almost all selected metal ions. This is consistent with the formation of 1:3 and 1:4 complexes found in the literature for diglycolamide-based ligands [32]. It has also been reported that, in the extracted species, the occurrence of 4 molecules of the extracting agent is associated with the formation of oligomeric forms of diglycolamide [42]. However, Pu and U deviate from the observed trend. Using a double methylated TDDGA, Verlinden et al. reported the same observation with respect to Pu and explained this by the possible role of its oxidation state. For the lanthanides, the slopes appear to increase slightly with their mass, going from La to Eu, which is in agreement with the literature [40]. Furthermore, a slight decrease in the slope value can be observed at the transition from Eu (m = 3.8) *via* Ho (m = 3.5) and Tm (m = 3.6) to Lu (m = 3.5).

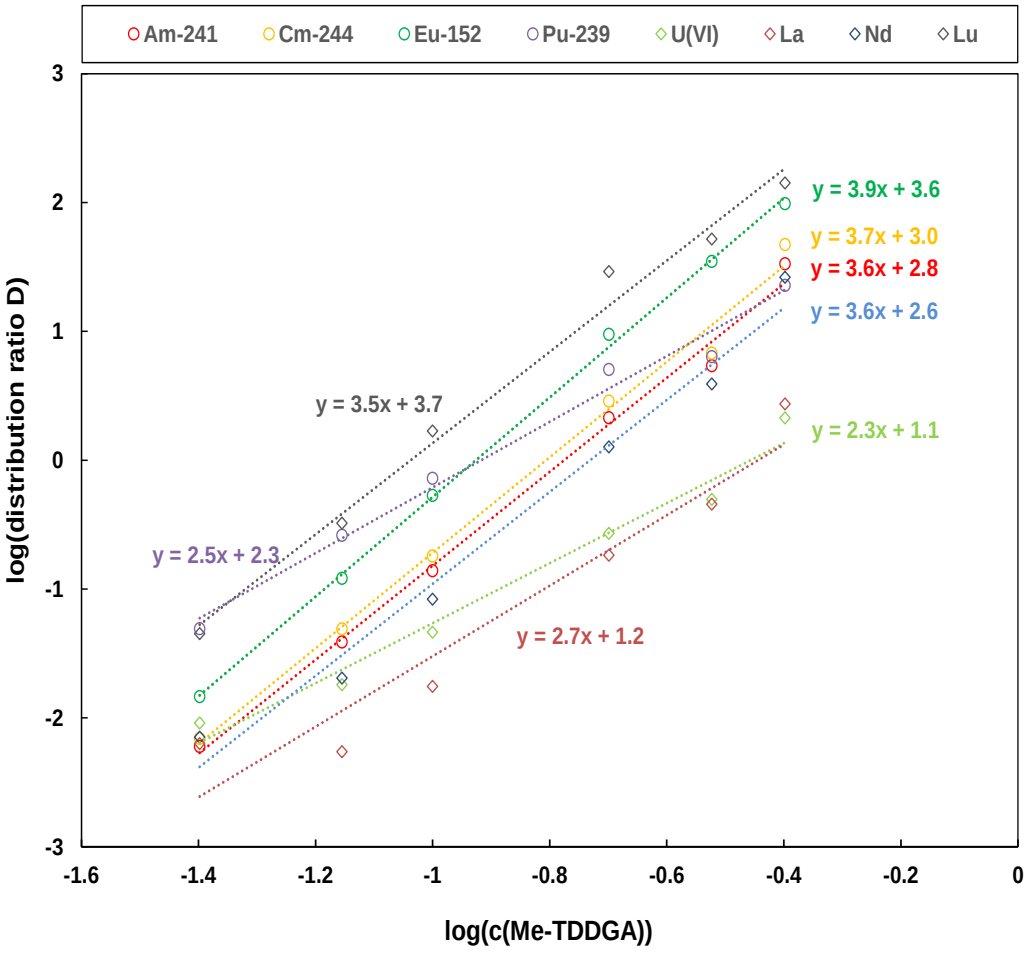

Figure 11: Slope analysis for the extraction of different metal ions by Me-TDDGA. Org.phase: different concentrations of the extractant (0.04-0.4 mol/L) in n-dodecane. Aq.phase: 1,079 mol/L HNO_3, 10^{-5} mol l/L Ln (III) (without Pm, +Y), ^{241}Am, ^{244}Cm, ^{152}Eu, ^{239}Pu, ^{237}Np, U-nat, t=30 min, T=22°C ± 1°C.

4.1.3 Temperature Dependence of Extraction

In this section, the temperature dependence of the distribution ratio values of various lanthanides and actinides using Me-TDDGA in a temperature range from 5 to 60°C is evaluated. No thermodynamic evaluation of the data was carried out, since this would require

further temperature-dependent data on nitric acid extraction. Figure 12 illustrates the distribution ratio for different metal ions as a function of temperature. It can be seen that the extraction of Am(III), Cm(III) and Eu(III) decreases with increasing temperature, indicating the exothermic nature of the extraction equilibria. The same trend was observed for Pu(IV) and U(VI), however, D appears to increase slightly for both elements at T = 35°C before decreasing again. Ansari et al. performed thermodynamic studies on the extraction of Pu(IV) and U(VI) with TODGA and observed a decrease in D values with increasing temperature for all data sets. The fact that U and Pu have different oxidation states than the other elements could explain why their extraction behaves differently. This could be a true temperature effect, but it is also possible that it is just an experimental error. Further verification through repeated experiments and speciation analysis would help to explain this behaviour.

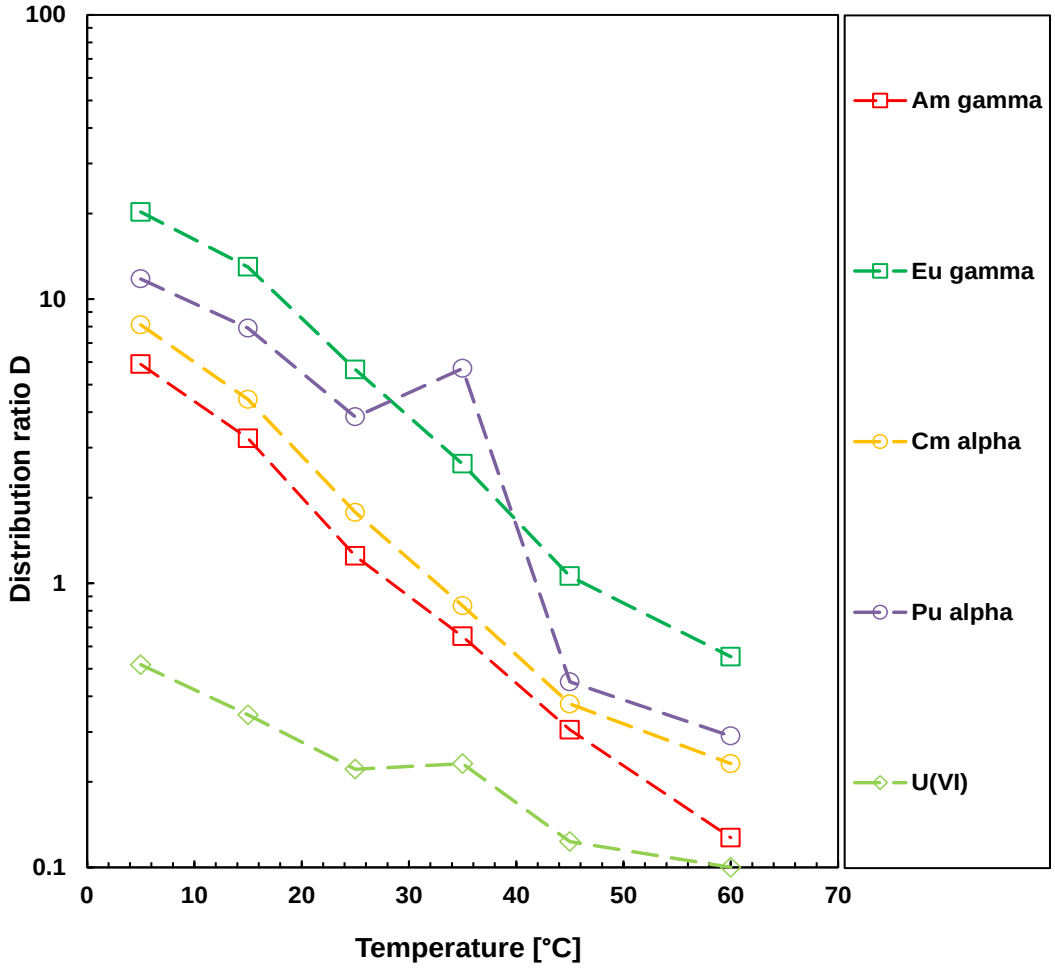

Figure 12: Distribution ratios of the various metal ions as a function of temperature [5-60°C]. Organic phase: from 0.2 mol/L Me-TDDGA in n-dodecane. Aqueous phase: 1,074 mol/L HNO_3, 10^{-5} mol/L Ln(III) (without Pm, +Y), ^{241}Am, ^{244}Cm, ^{152}Eu, ^{239}Pu, ^{237}Np, U-nat, t=30 min.

The temperature dependence of SF was also investigated for different metal ions as shown in Table 2. The $SF_{Eu/Am}$ values remain relatively constant over the entire temperature range and lie between 3.5 and 4.5, which indicates that Eu is better extracted than Am. For $SF_{Cm/Am}$, the values up to T = 60°C are relatively stable at 1.3-1.4, which consistently indicates a low selectivity of Cm over Am. A clear and unambiguous trend can be observed for $SF_{Am/U}$, where the values drop significantly with increasing temperature. The values are above 1 and indicate

a good extraction of Am compared to U. Inconsistent values are observed for $SF_{Am/Pu}$, where the values almost alternately decrease and increase, reaching the highest value at higher temperatures T = 45°C. Further experimental verification steps are required to determine the influence of temperature on Pu(IV) extraction. Furthermore, Sharov et al. [42] detected a similar effect in the extraction of Am(III), Eu(III) and Lu(III) with TODGA in a mixture of *n*-dodecane and 1-decanol in 1 M HNO_3. For different TODGA concentrations, inflection points or plateaus were observed in the temperature range from 15 to 25°C, where the distribution ratio values increased. They explained this anomalous dependence by the formation of different extracted species of the considered metals at different temperatures [42].

Table 2: Separation factors $SF_{M/Am}$ (M=Eu, Cm, Pu) and $SF_{Am/U}$ for extractions with 0,2 mol/L Me-TDDGA in n-dodecane and 1.074 mol/L HNO_3 including 10^{-5} mol/L Ln(III) (without Pm and Y) at different temperature values (5-60°C), t=30min.

	c(HNO_3) = 1.074 mol/L, c(Me-TDDGA) = 0.2 mol/L			
T(°C)	**$SF_{Eu/Am}$**	**$SF_{Cm/Am}$**	**$SF_{Pu/Am}$**	**$SF_{Am/U}$**
5	3.4	1.4	1.6	11.4
15	4.0	1.3	2.0	9.4
25	4.5	1.4	2.5	5.6
35	4.0	1.2	6.2	2.8
45	3.5	1.4	1.7	2.5
60	4.3	1.3	1.5	1.3

The extraction of the lanthanide series (w/o Pm +Y) was studied using solutions of all Ln(III) at different temperatures (5-60°C), as shown in Figure 13. The distribution ratio decreases with increasing temperature values, confirming the exothermic nature of the extraction. Due to the lanthanide contraction phenomenon, the distribution values increase within the elements and reach a maximal value at Er or Tm before slightly decreasing for the rest of the series elements.

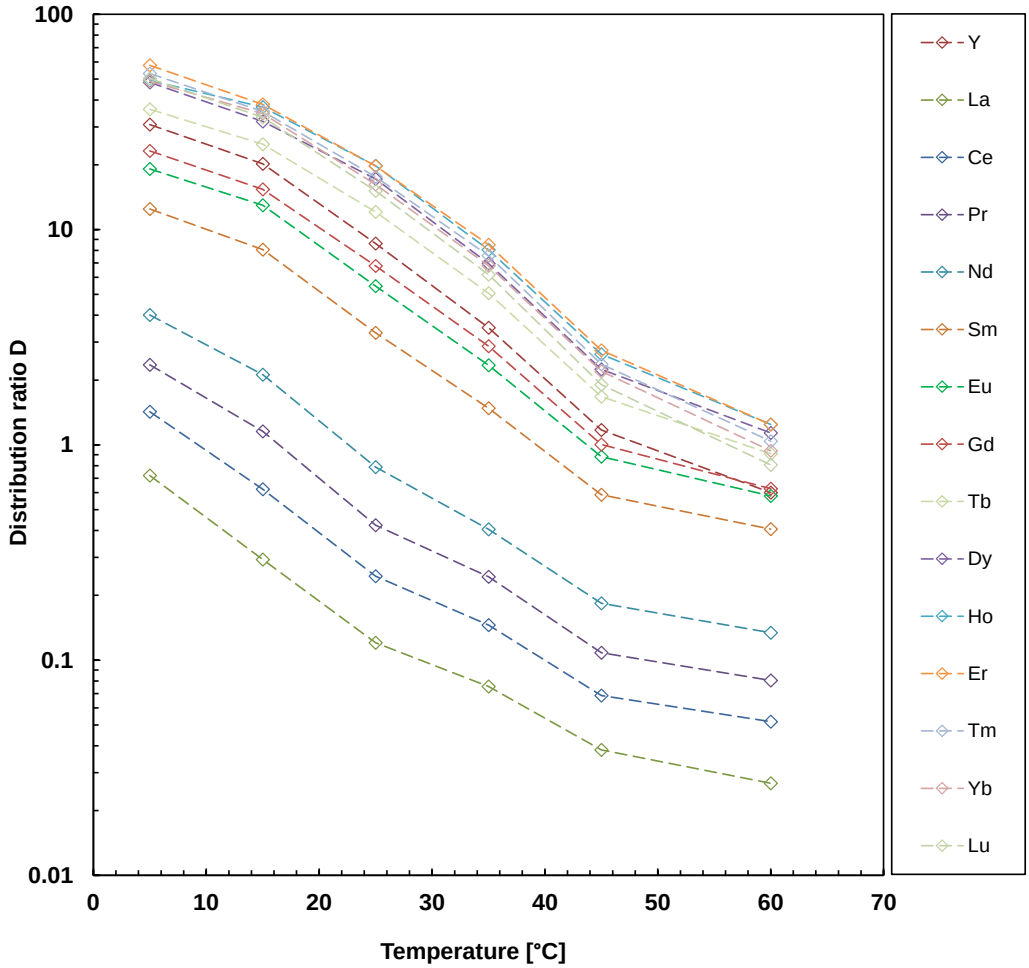

Figure 13: Distribution ratios of lanthanides as a function of temperature [5-60°C]. Organic phase: from 0.2 mol/L Me-TDDGA in n-dodecane. Aqueous phase: 1,074 mol/L HNO_3, 10^{-5} mol/L Ln(III) (without Pm, +Y), ^{241}Am, ^{244}Cm, ^{152}Eu, ^{239}Pu, ^{237}Np, U-nat, t=30 min.

4.1.4 Extraction Kinetics

Extraction kinetics studies of selected metal ions were carried out to determine the equilibration time. Distribution ratio values were plotted against contact time ranging from 1 to 60 minutes, as illustrated in Figure 14. The obtained plot shows that the kinetics of the extraction system is fast. All elements seem to reach equilibrium within the first 5 to 10 minutes and stabilize over time. Eu(III) showed the highest distribution values (about 10), while U(VI) showed the lowest values (about 0.3). The graph also shows a slight decrease in Pu distribution ratios over time, rather than reaching a plateau as observed for other elements, indicating a possible change in the oxidation state of Pu in solution. Verlinden et.al. reported a similar effect for Pu(IV) and Np(V) and explained it by the fact that these elements undergo changes in metal ion speciation [40].

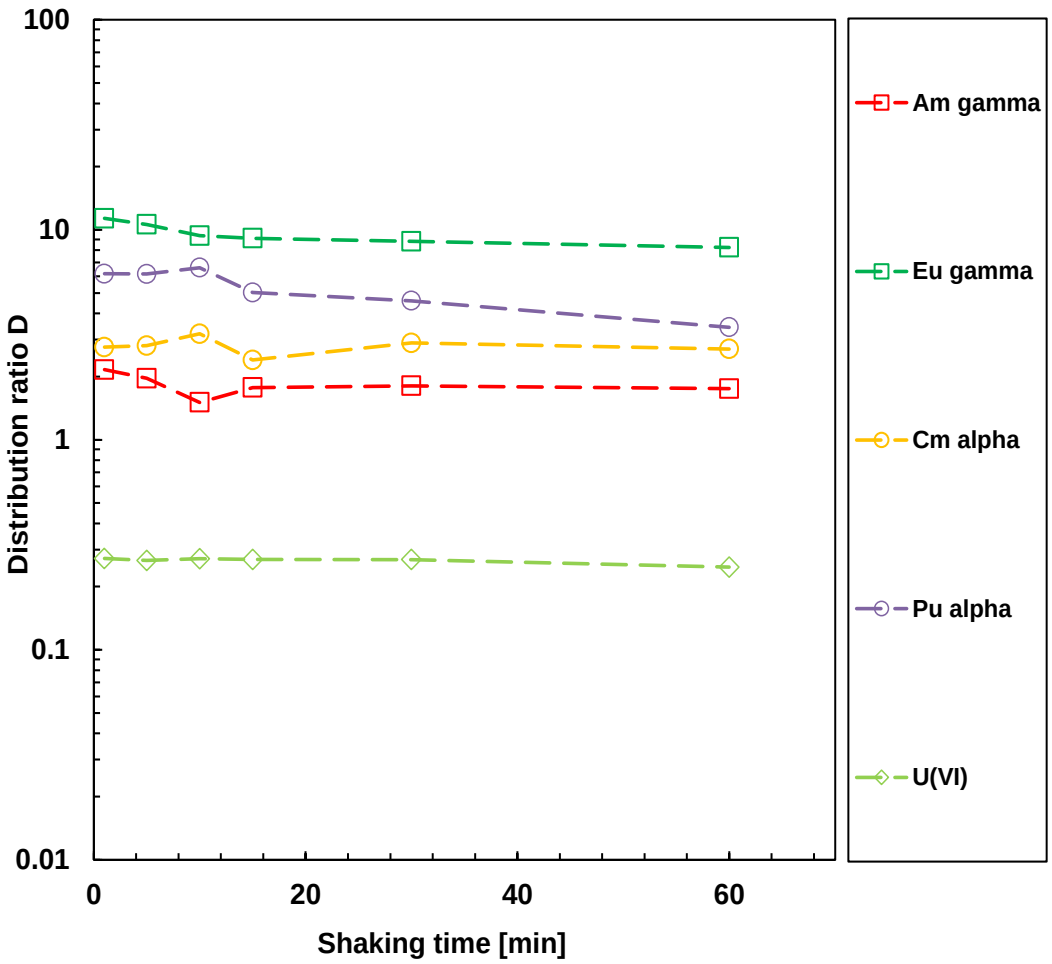

Figure 14: Distribution ratios of various metal ions as a function of contact time (1-60 minutes). Organic phase: from 0.2 mol/L Me-TDDGA in n-dodecane. Aqueous phase: 1,074 mol/L HNO_3, 10^{-5} mol/L Ln(III) (without Pm, +Y), ^{241}Am, ^{244}Cm, ^{152}Eu, ^{239}Pu, ^{237}Np, U-nat, T=22°C± 1°C, mixing time t=30 min.

Table 3 shows selectivity patterns for the separation of Am from various elements as a function of time. The separation factor $SF_{Eu/Am}$ is consistently above 1 and remains relatively stable (around 5 and 6), indicating a preference for Eu extraction over Am extraction, as is also found in the sections above. The values of $SF_{Cm/Am}$ remained almost constant at the value 1.40 reached in the first minute, although the slight decrease over time resulted in it being between 1.36 and 1.39. Once again, Cm is lightly better extracted than Am. In addition, the data show that Am is extracted selectively over U, as indicated by the $SF_{Am/U}$ values, which are well above 1, and that Pu is preferentially extracted over Am.

Although this could also be the result of experimental fluctuations, a drop in all SFs at different time points of the extraction might indicate a change in speciation of the metals or the presence of other ligand-metal interactions competing with the thermodynamically or/and kinetically favourable complexes. In the slope analysis, 1:4 was the predominant stoichiometry, which is associated with the formation of oligomeric forms of diglycolamide, indicating the coexistence of several extracted species with different ligand:metal ratios. According to reference [42], in the case of Am(III) and Eu(III), a transition from compounds with 2 TODGA molecules per 1 metal atom to compounds with 3 TODGA molecules is observed with increasing temperature. Maybe this could also be the case as the contact time increases. In the case of Am(III) and

Eu(III), a transition from compounds with 2 TODGA molecules per 1 metal atom to compounds with 3 TODGA molecules is observed with increasing temperature. A similar transition may occur as the contact time increases, leading to the formation of new extracted species with different configuration.

Table 3: Separation factors $SF_{M/Am}$ (M=Eu, Cm, Pu) and $SF_{Am/U}$ for extractions with 0.2 mol/L Me-TDDGA in n-dodecane and 1.074 mol/L HNO_3 including 10^{-5} mol/L Ln(III) (without Pm and Y), T = 22°C ± 1°C, mixing time t=30 min.

	c(HNO_3) = 1.074 mol/L, c(Me-TDDGA) = 0.2 mol/L			
Shaking time (min)	**$SF_{Eu/Am}$**	**$SF_{Cm/Am}$**	**$SF_{Pu/Am}$**	**$SF_{Am/U}$**
1	5.25	1.40	3.11	7.93
5	5.40	1.36	2.99	7.38
10	6.22	1.39	2.87	5.55
15	5.14	1.36	2.85	6.59
30	4.88	1.36	2.16	6.72
60	4.71	1.37	1.73	7.08

To illustrate the influence of the contact time on the lanthanide extraction behaviour, the distribution ratios were plotted against the contact time. Figure 15 shows that all lanthanides exhibit similar behaviour, with the maximum appearing to be reached in 10 minutes, followed by a decrease in D values at t~ 15min and a rise again, which remains stable over time. The decrease in D values becomes more pronounced for the medium and especially the heavy lanthanides, as the distribution ratio for Ho, for example, decreases from 30 at t = 10 min to 14 at t = 30 min. As previously described above with other parameters (acid and ligand concentrations, and temperature effect), the distribution ratio values increase until they reach a maximum at Er(III), at t = 10 min, and then fall slightly for the rest of the heavy lanthanides.

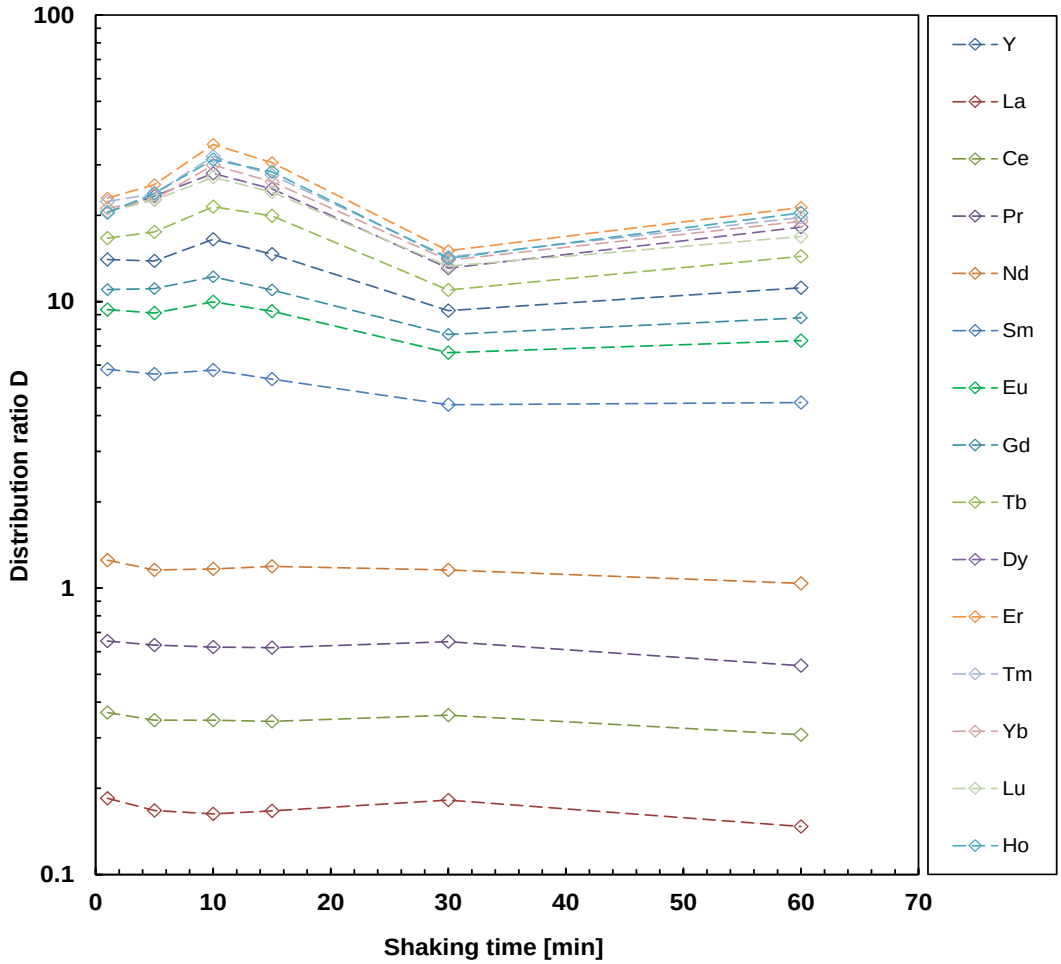

Figure 15: Distribution ratios of lanthanides as a function of contact time (1-60 minutes). Organic phase: from 0.2 mol/L Me-TDDGA in n-dodecane. Aqueous phase: 1,074 mol/L HNO_3, 10^{-5} mol/L Ln(III) (without Pm, +Y), ^{241}Am, ^{244}Cm, ^{152}Eu, ^{239}Pu, ^{237}Np, U-nat, T=22°C± 1°C, mixing time t=30 min.

4.2 Organic Phase Loading

A significant concern with DGA extractants dissolved in aliphatic diluents is their tendency to form a third phase when in contact with solutions containing nitric acid and metal ions in high concentrations. To assess the loading capacity of the extraction system, two main concepts are used: the limited organic concentration (LOC) and the critical aqueous concentration (CAC). While the maximum metal ion concentration in the initial aqueous phase without splitting the organic phase into two phases is referred to as CAC, the corresponding metal ion concentration in the organic phase is referred to as LOC. Graphically, the point above which the organic Nd(III) concentration drops sharply was defined as the LOC. Higher LOC and CAC values are indicative of higher loading capacities and a lower likelihood of third phase formation. Several parameters such as HNO_3 concentration, metal ions, extractant concentration and temperature can influence the formation of a third phase in the extraction system [43].

4.2.1 Nd(III) Loading

Due to its similar physical and chemical properties to Am(III) and Eu(III), Nd(III) is often used as an equivalent to these metal ions to study the extractability of extractants and to investigate the formation of a third phase in the extraction system [43]. In the present experiment, it was

possible to clearly recognize the appearance of the second organic phase after centrifugation by eye, as shown in Figure 16.

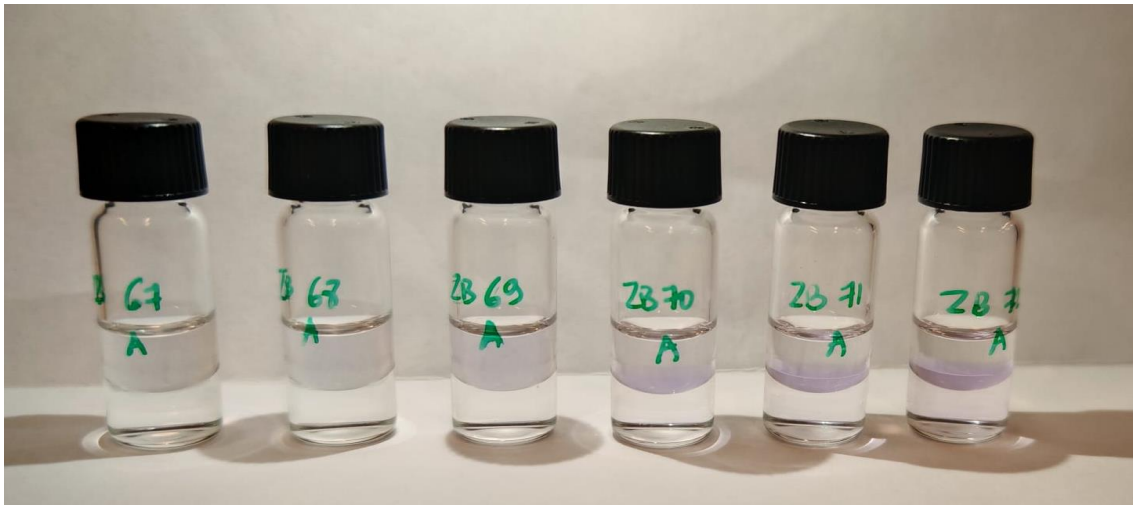

Figure 16: Samples after centrifugation, extraction series with 0.2 mol /L Me-TDDGA in n-dodecane and HNO_3 with different Nd(III) concentrations (0.01, 0.02, 0.04, 0.06, 0.08 and 0.1 mol/L from left to right), , T=22±1 °C, mixing time t=30 min.

Figure 17 displays the organic equilibrium concentration of Nd(III), $[Nd]_{org.}$ for 0.2 mol/L Me-TDDGA in *n*-dodecane as a function of the initial aqueous concentration of Nd(III), $[Nd]_{ini.}$, ranging from 0.01 to 0.1 mol/L in 2.236 mol/L HNO_3. The $[Nd^{3+}]_{org.}$ reached a maximum at a value of ca. 0.068 mol/L after which it dropped drastically, indicating the formation of the third phase. According to slope analysis performed in 4.1.2, the stoichiometry of the Nd–Me-TDDGA complex is 1:3 in the organic phase, the maximum loading capacity of 0.2 mol/L Me-TDDGA should be about 0.067 mol/L, which corresponds to the value obtained experimentally. In addition, the distribution ratio of Nd(III) increases with increasing Nd(III) concentration for the first two concentrations, before decreasing significantly for the remaining concentrations.

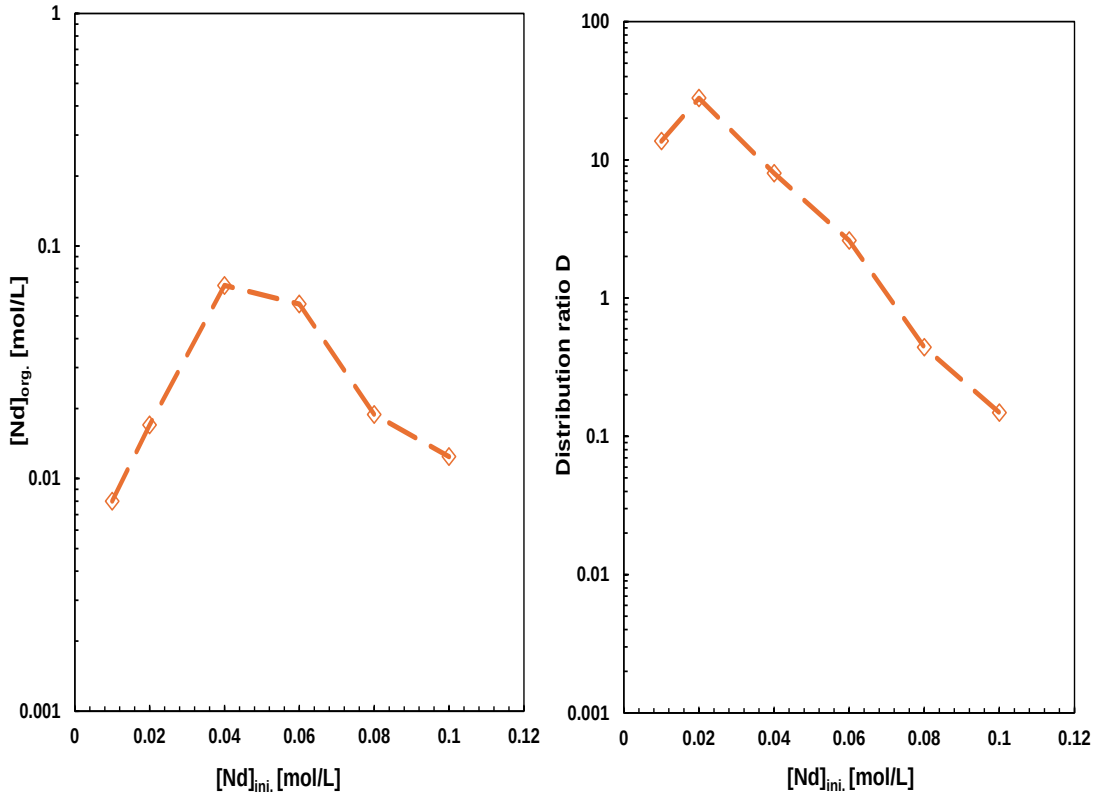

Figure 17: Organic phase concentrations for Nd(III) (left) and distribution ratios and (right) plotted against initial Nd(III) concentration in the aqueous phase for solvent composition 0.2 mol/L Me-TDDGA in n-dodecane. Aqueous phase: different Nd(III) concentrations in 2.236 mol/L HNO_3, T=22±1 °C, mixing time t=30 min.

4.2.2 Th(IV) Loading

Thorium in its tetravalent state was selected as a representative element of the actinide series to investigate the loading capacity of Me-TDDGA towards tetravalent actinides. In contrast to Nd(III) solutions, which were slightly coloured, Th(IV) solutions were clear, and it was difficult to clearly visualize the appearance of the second organic phase by eye after centrifugation, as shown in Figure 18. However, a thick and highly viscous phase formed as the third phase, which made it difficult to take a sample from the light organic phase.

Figure 19 shows the equilibrium organic concentration of Th(IV), $[Th]_{org.}$ for 0.2 mol/L Me-TDDGA in *n*-dodecane as a function of the initial aqueous concentration of Th(IV), $[Th]_{ini.}$, ranging from 0.01 to 0.6 mol/L in 2.2 mol/L HNO_3. The $[Th]_{org.}$ achieved a maximum at a value of about 0.068 mol/L, after which it dropped drastically, indicating the formation of the third phase. Assuming that the stoichiometry of the Th-Me-TDDGA complex in the organic phase is 1:3, the maximum loading capacity of 0.2 mol/L Me-TDDGA should be about 0.067 mol/L, which is consistent with the experimentally obtained value.

In literature [44], the distribution ratio of Th(IV) was found to increase progressively with increasing Th(IV) until it drops significantly, indicating the formation of a third phase. In contrast, distribution ratio values in Figure 19 were relatively stable and decreased dramatically

when the LOC was reached. This could be due to the coexisting Th(IV) species or the change in the 1:3 stoichiometry of the Th-Me-TDDGA complex.

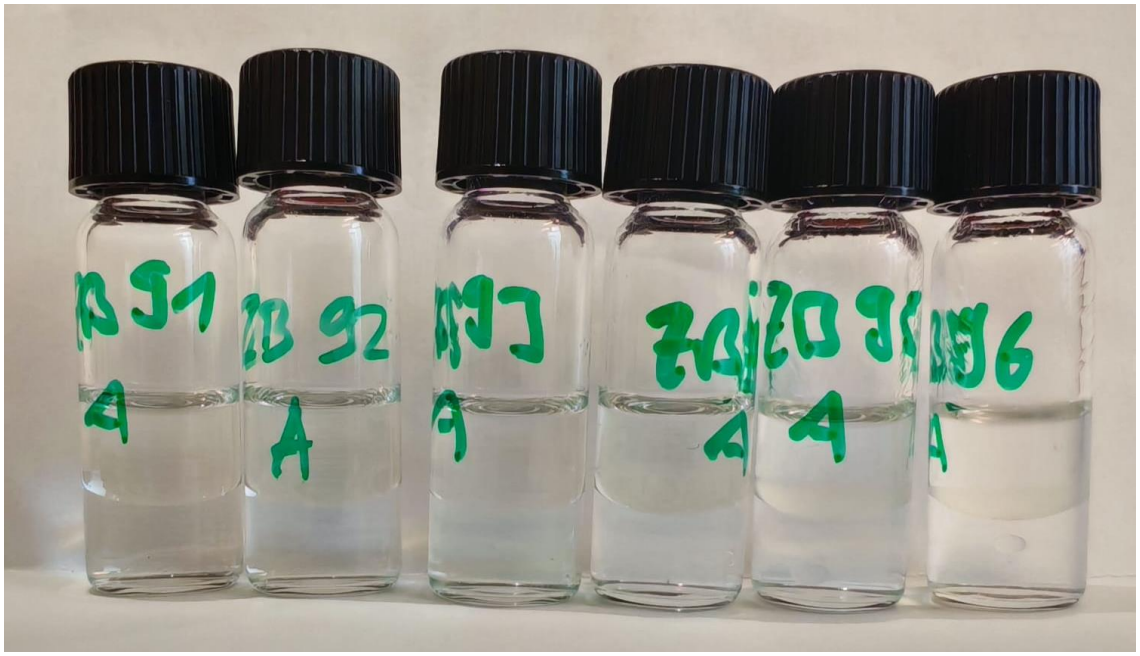

Figure 18: Samples after centrifugation, extraction series with 0.2 mol /L Me-TDDGA in n dodecane and 2.236 mol/L HNO_3 with different Th(IV) concentrations (0.01, 0.02, 0.03, 0.04, 0.05 and 0.06 mol/L from left to right).

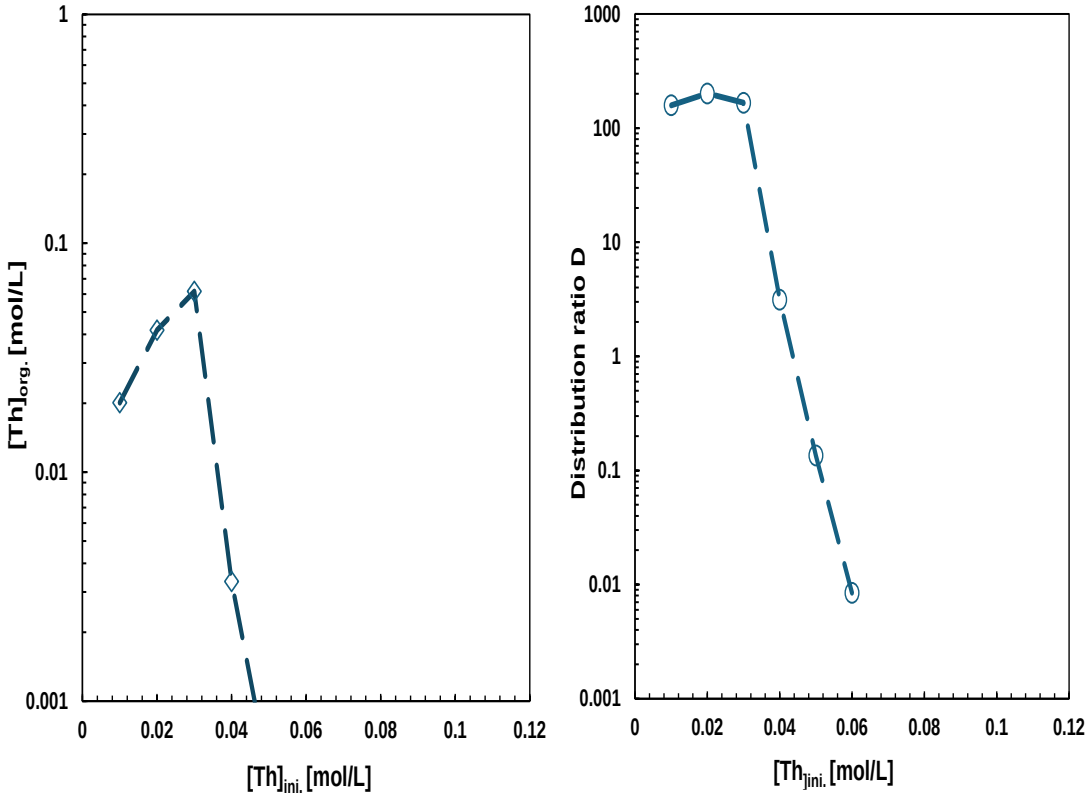

Figure 19: Organic phase concentrations for Th(IV) (left) and distribution ratios and (right) plotted against initial Th(IV) concentration in the aqueous phase for solvent composition 0.2 mol/L Me-TDDGA in n-dodecane. Aqueous phase: different Th(IV) concentrations in 2.236 mol/L HNO_3, T=22±1 °C, mixing time t=30 min.

4.3 Combined Extraction Systems

In this section, the effect of two water-soluble co-extractants, SO_3-Ph-BTP and PTD, on the selectivity towards An(III) and Ln(III) will be investigated in the presence of the main DGA ligand, Me-TDDGA. For both experiments, the nitric acid concentration was varied from 0.052 to 3.38 mol/L. The distribution ratio and SF values are to be compared with the previous system in which only Me-TDDGA was used.

4.3.1 Me-TDDGA and SO_3-Ph-BTP

Figure 20 shows the phase separation after centrifugation, with distinct organic and aqueous phases. The greenish color of the aqueous phase is due to SO_3-Ph-BTP dissolved in nitric acid. No precipitation or third-phase formation was observed. The corresponding distribution ratios D are illustrated below in Figure 21.

The introduction of SO_3-Ph-BTP led to a significant decrease in the distribution ratios of all metal ions, especially Am(III) and Eu(III), with Am(III) being more affected. For example, at a concentration of 1.074 mol/L nitric acid, D(Am(III)) decreases from 2.3 in the absence of SO_3-Ph-BTP to 0.008 when SO_3-Ph-BTP was added, while D(Eu(III)) drops from 10.3 to 3.1. As expected, the distribution ratio values increased with increasing nitric acid concentration, and higher distribution ratio values were obtained for Pu(IV) and Cm(III) at the highest HNO_3 concentration (3.38 mol/L): it increases from 11 with only Me-TDDGA to 33.8 in the presence of SO_3-Ph-BTP and from 17.10 to 37.60, for Pu(IV) and Cm(III), respectively. For U(VI), the distribution ratio values appear to be relatively stable in the presence of SO_3-Ph-BTP.

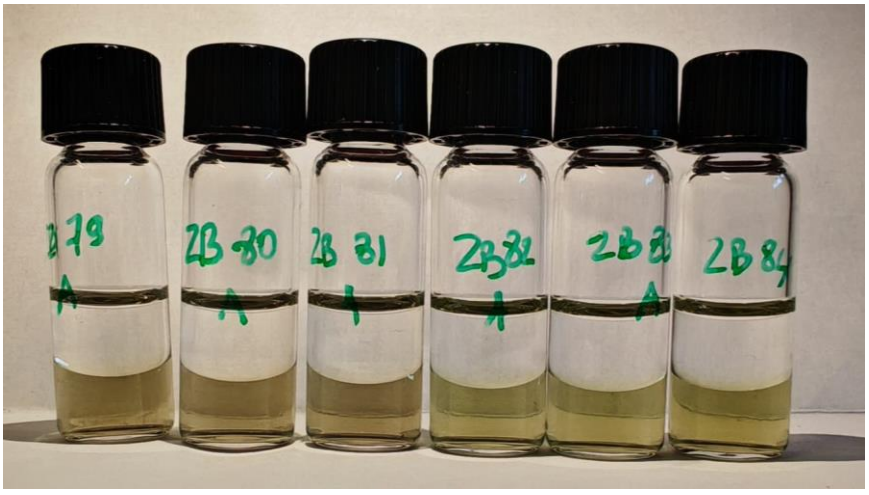

Figure 20: Samples after centrifugation, extraction series with 0.02 mol/L SO_3-Ph-BTP in nitric acid. Organic phase: 0.2 mol/L Me-TDDGA in n-dodecane. Aqueous phase: 0.02 mol/L SO_3-Ph-BTP, 0.052 to 3.38 mol/L HNO_3, 10^{-5} mol/L Ln(III) (without Pm and Y) and ^{41}Am, ^{244}Cm, ^{152}Eu, ^{239}Pu, ^{237}Np, U-nat , T = 22°C ± 1°C, mixing time t=30 min.

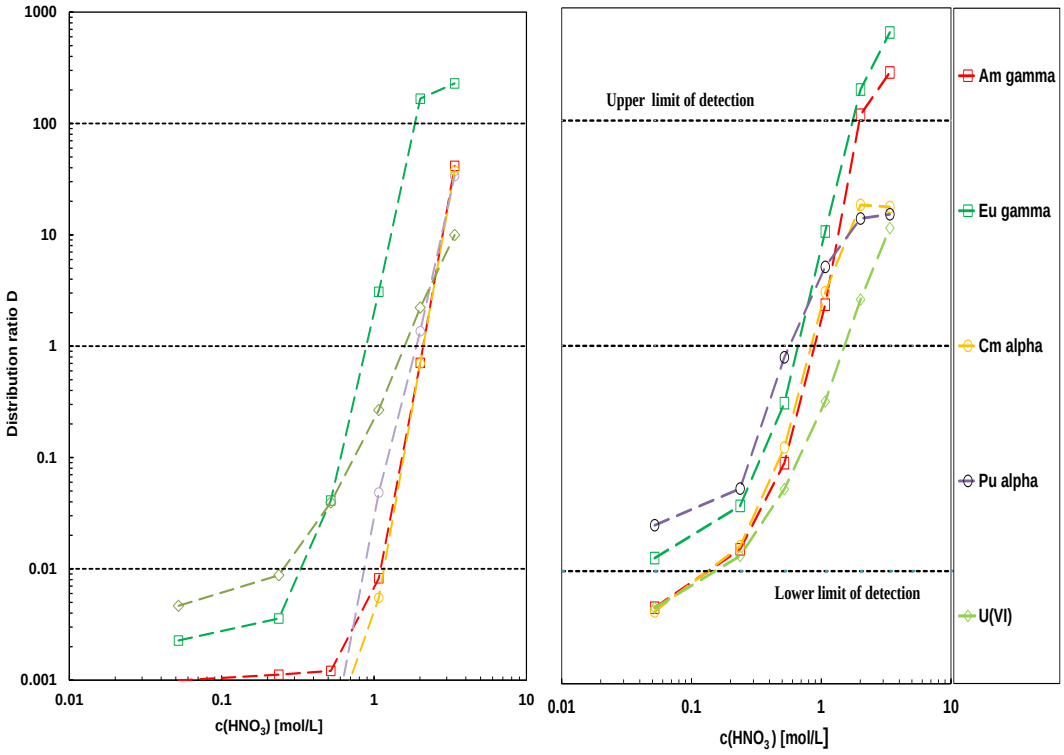

Figure 21: Distribution ratios of different metal ions with 0.02 mol/L SO_3-Ph-BTP (left), without SO_3-Ph-BTP (right) as a function of the HNO_3 concentration. Organic phase: 0.2 mol/L Me-TDDGA in n-dodecane. Aqueous phase: 0.02 mol/L SO_3-Ph-BTP, 0.052 to 3.38 mol/L HNO_3, 10^{-5} mol/L Ln(III) (without Pm and Y) and ^{241}Am, ^{244}Cm, ^{152}Eu, ^{239}Pu, ^{237}Np, U-nat, T = 22°C ± 1°C, mixing time t=30 min.

The water-soluble form SO_3-Ph-BTP was found to form stronger complexes with Am(III) than the lanthanide ions [45]. In the first extraction system using only Me-TDDGA, the $SF_{Eu/Am}$ values were all below 10, with the maximum $SF_{Eu/Am}$ value being 4.5 at $c(HNO_3)$ = 1.074 mol/L, indicating a low selectivity of Eu(III) over Am(III). In the presence of SO_3 Ph-BTP, the D(Am(III)) value decreased by several orders of magnitude (a fall from 2.317 to 0.008 when SO_3-Ph-BTP was introduced), leading to a significant increase in $SF_{Eu/Am}$ values up to few hundreds, as shown in Table 4. However, the $SF_{Eu/Am}$ decreased with increasing nitric acid concentration, reaching 5.5 at $c(HNO_3)$ = 3.38 mol/L. A similar effect has been observed in the literature, the decrease in these SF values at higher acidity is mainly due to the increased distribution ratio values of Am(III), as the protonation of SO_3-Ph-BTP at higher acidity reduces its effective complexing ability [45].

Since $SF_{Am/Cm}$ is barely above 1, the extraction selectivity between Am and Cm is weak, and they are almost equally distributed between the organic and aqueous phase, although Am(III) can be extracted marginally better than Cm(III). This contrasts with literature results [23] where Cm(III) is extracted slightly better than Am(III) in the presence of BTP ligands. A corresponding trend was observed by Geist et al. [46], where the distribution ratios of Am(III) and Cm(III) were relatively equal. This was explained by a compensation effect, where TODGA and BTP effects cancel each other out, resulting in a reduced overall separation. As for Pu(IV), the highest $SF_{Am/Pu}$ value was 1.23, again suggesting that the selectivity of Am(III) over Pu(IV) is low, as the highest $SF_{Am/Pu}$ value is slightly higher than 1.

Table 4: Separation factors $SF_{Am/M}$ (M=Eu, Cm, Pu, U) for extractions with 0.2 mol/L Me-TDDGA in n-dodecane and 0.02 mol/L SO_3-Ph-BTP in different HNO_3 concentrations, including 10^{-5} mol/L Ln(III) (without Pm and Y), ^{41}Am, ^{244}Cm, ^{152}Eu, ^{239}Pu, ^{237}Np, U-nat, T = 22°C ± 1°C, mixing time t=30 min.

	c(Me-TDDGA)=0.2 mol/L, c(SO_3-Ph-BTP)=0.02 mol/L			
c(HNO_3) [mol/L]	**$SF_{Eu/Am}$**	**$SF_{Am/Cm}$**	**$SF_{Am/Pu}$**	**$SF_{Am/U}$**
0.052	-	-	-	-
0.237	-	-	-	-
0.58	33.95	-	-	0.03
1.074	374.36	-	0.17	0.03
2.009	235.70	1.01	0.52	0.20
3.38	5.50	1.11	1.23	4.20

As for the extraction behavior of the lanthanides in the presence of Me-TDDGA and SO_3-Ph-BTP while varying the HNO_3 concentration, Figure 22 shows the distribution ratio of the different elements as a function of HNO_3 concentration. When the HNO_3 concentration increases, the D values for each element also increase, with the maximum D value corresponding to the highest nitric acid concentration. Compared with the previous extraction system using only Me-TDDGA, the distribution ratio values in the combined extraction system are relatively lower for the light lanthanides, while they decrease significantly for the heavy lanthanides. For example, D(Ho(III)) at c(HNO_3)=1.074 mol/L decreases from 27.8 to 0.4 when SO_3-Ph-BTP is introduced. To investigate the influence of lanthanide contraction on the distribution ratio values, these were plotted against the inverse ionic radius for each element, as shown in Figure 23. It can be seen that the distribution ratio values increase for the light lanthanides, from La to Sm, and gradually decrease for the medium and heavy lanthanides, with D values below 1 for the heavy lanthanides. Thus Sm(III) has the highest distribution ratio and Lu(III) the lowest. This can be seen visually in Figure 23, where the curve reaches its maximum at Sm(III). In contrast, Y(III), which behaves like a heavy lanthanide due to its large ionic radius, has a high D value of roughly 6.1. Furthermore, a clear separation of Cm(III)+Am(III) from the following relevant lanthanides (Nd, Sm, Gd, +Y), which are considered neutron poisons, is possible, since these elements D(Ln(III)) > 1, D(Am(III)) < 1 at c(HNO_3)=1.074 mol/L.

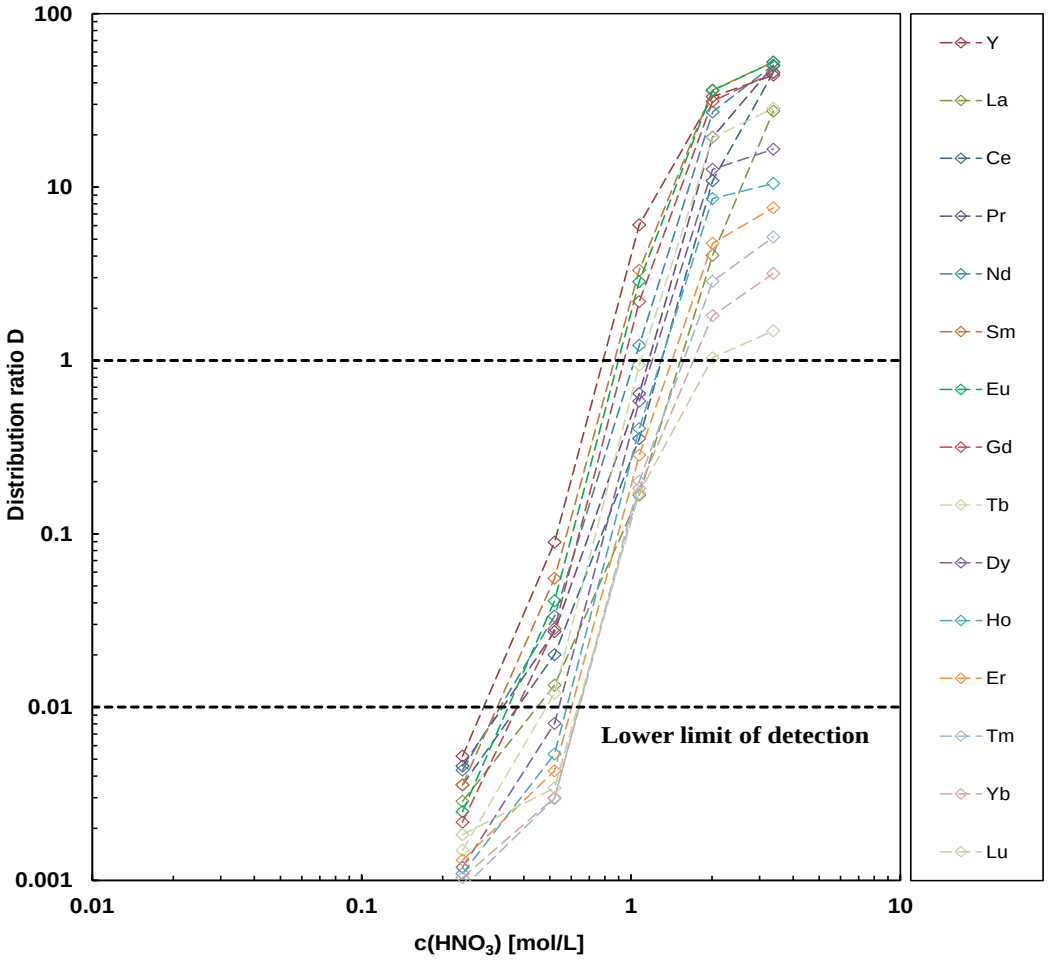

Figure 22: Distribution ratios of Ln(III) (without Pm, +Y) as a function of HNO_3 concentration for extraction with 0.2 mol/L Me-TDDGA in n-dodecane and 0.02 mol/L SO_3-Ph-BTP.

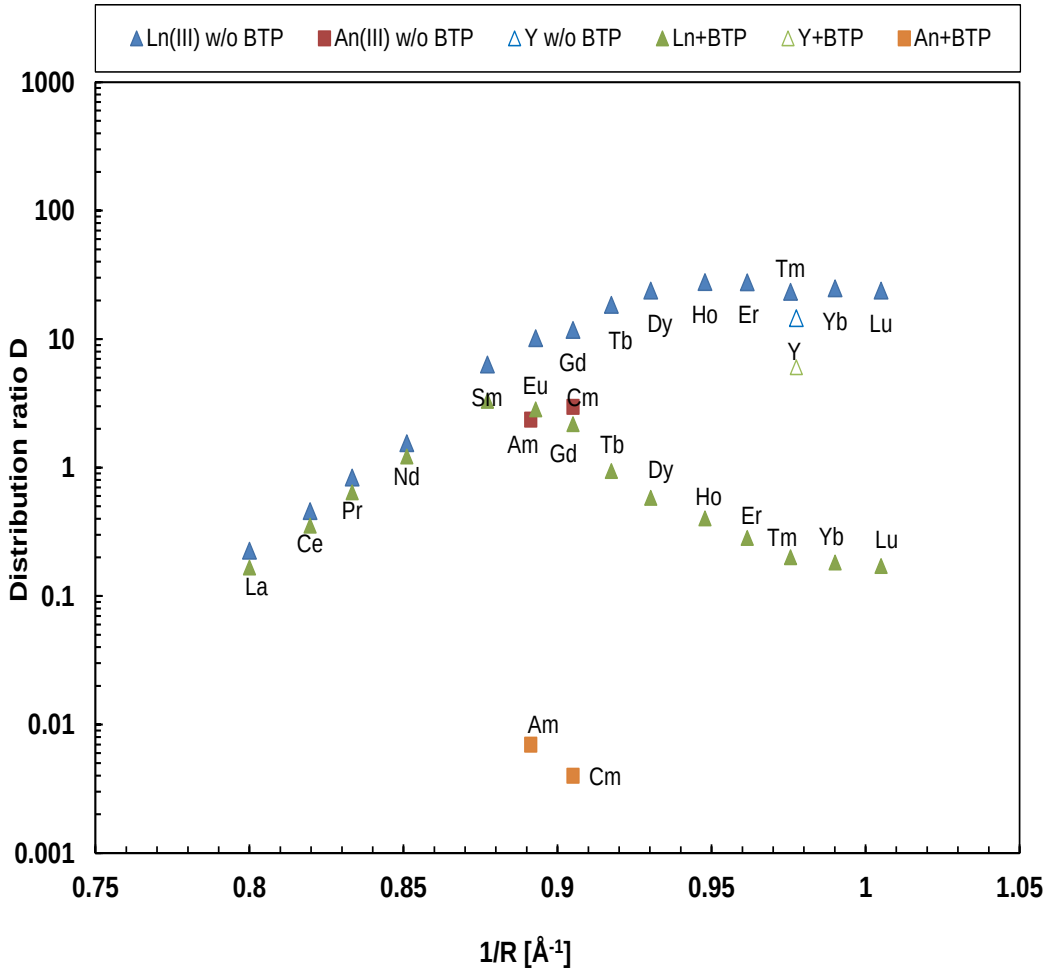

Figure 23: Distribution ratios of Am(III), Cm(III) and Ln(III) (without Pm, +Y,) as a function of the inverse radius with 0.2 mol/L Me-TDDGA in n-dodecane, in the presence and the absence of SO_3-Ph-BTBP (0.02 mol/L) in 1.074 mol/L HNO_3.

4.3.2 Me-TDDGA and PTD

In contrast to SO_3-Ph-BTP, PTD contains only C, H, O and N atoms, making it completely incinerable, and it has been reported to be highly selective for An(III). To investigate its extractability, 0.02 mol/L PTD was prepared in different concentrations of HNO_3 (Figure 24), while the organic phase was kept unchanged with 0.2 mol/L Me-TDDGA in n-dodecane. Figure 25 shows the distribution ratios for different metal ions in the presence and absence of PTD as co-extractant. As expected, the D values for all metal ions increase with increasing HNO_3 concentration. At the same time, the D values are slightly lower than those obtained using Me-TDDGA alone. Eu(III) appears to be less affected by the decrease compared to Am(III). For Cm(III) and Pu(IV), the D values improve at high HNO_3 concentrations. Again, the D values for U(VI) appear to be slightly unchanged despite the introduction of PTD. In the previous combined extraction system with SO_3-Ph-BTP, the selectivity towards An(III) was higher than in this system.

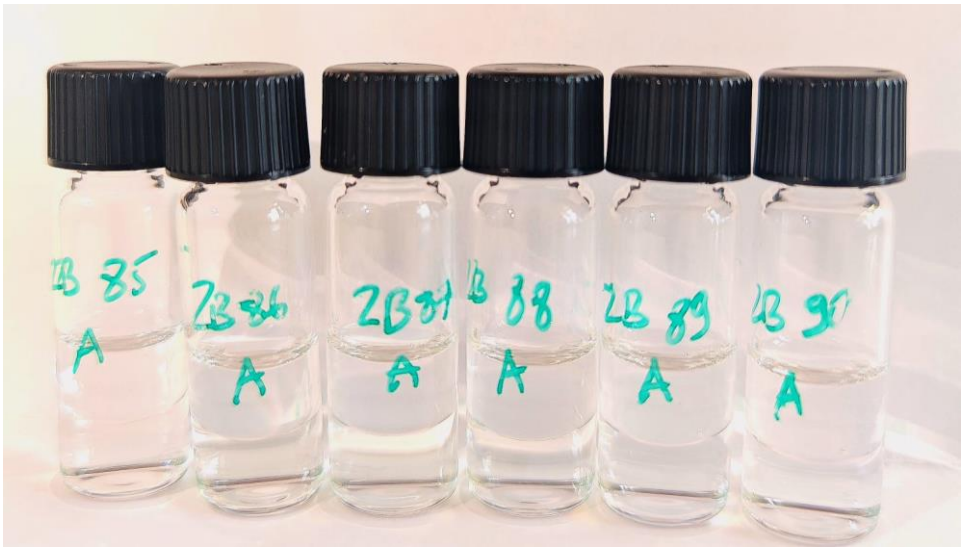

Figure 24: Samples after centrifugation, extraction series with 0.02 mol/L PTD in nitric acid. Organic phase: 0.2 mol/L Me-TDDGA in n-dodecane. Aqueous phase: 0.02 mol/L SO_3-Ph-BTP, 0.052 to 3.38 mol/L HNO_3, 10^{-5} mol/L Ln(III) (without Pm and Y) and ^{41}Am, ^{244}Cm, ^{152}Eu, ^{239}Pu, ^{237}Np, U-nat, T = 22°C ± 1°C, mixing time t=30 min.

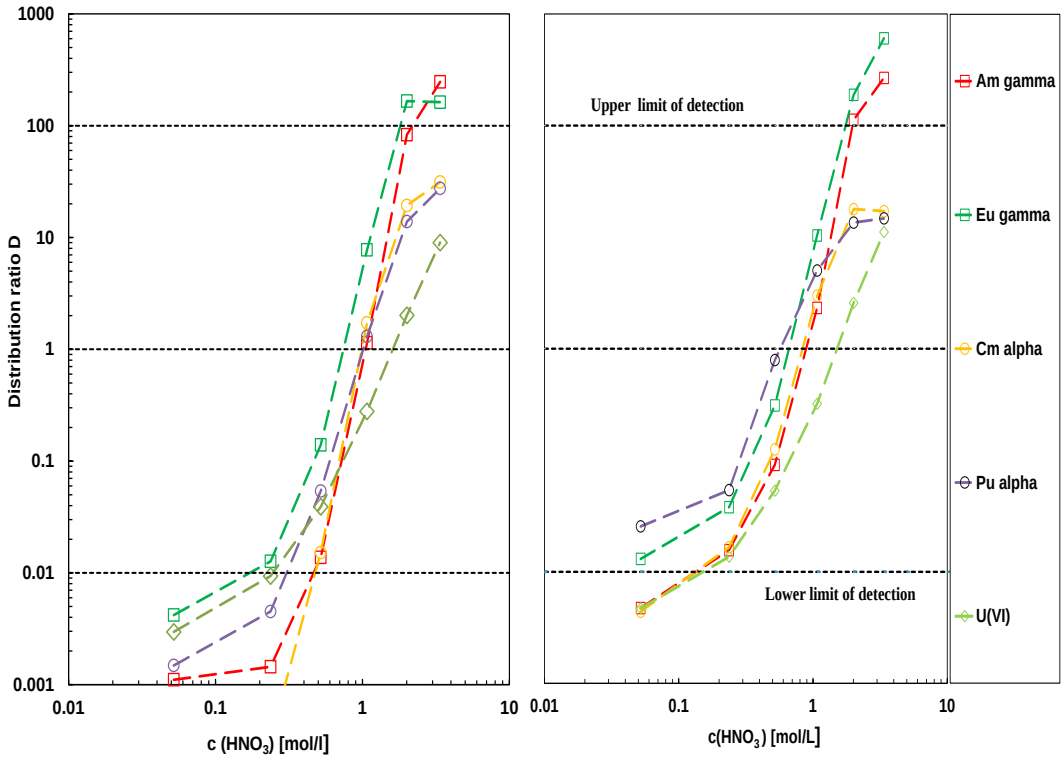

Figure 25: Distribution ratios of different metal ions with 0.02 mol/L PTD (left), without PTD (right) as a function of the HNO_3 concentration. Organic phase: 0.2 mol/L Me-TDDGA in n-dodecane. Aqueous phase: 0.02 mol/L PTD, 0.052 to 3.38 mol/L HNO_3, 10^{-5} mol/L Ln(III) (without Pm and Y)and ^{41}Am, ^{244}Cm, ^{152}Eu, ^{239}Pu, ^{237}Np, U-nat, T = 22°C ± 1°C, mixing time t=30 min-

To assess the selectivity of PTD towards different metal ions, the separation factors were calculated and presented in Table 5. Surprisingly, the $SF_{Eu/Am}$ are significantly lower than expected and reported in the literature, where the introduction of PTD with a DGA ligand yields a $SF_{Eu/Am}$=100 [47]. The highest $SF_{Eu/Am}$ achieved is 10.14 with c(HNO_3)=0.58 mol/L before

SF values decrease with increasing HNO_3. Furthermore, no relevant Am(III)/Cm(III) selectivity was observed, as both relevant $SF_{Cm/Am}$ values are slightly greater than 1. The $SF_{Cm/Am}$ values decrease again with increasing HNO_3 concentration. This decline in separation ability with increasing HNO_3 concentration is also observed for hydrophilic BTPs (SO_3-Ph-BTP for example, in section 3.4.1 above), BTBP, BTPhen and is attributed to the increase in the degree of ligand protonation and hence the decrease in free ligand concentration [47]. While all metal ions follow this trend, $SF_{Am/Pu}$ seems to increase with increasing HNO_3 concentration. It is possible that the protonated form of PTD preferentially complexes Pu(IV) over An(III), so further experiments are needed to confirm Pu(IV) extraction in the presence of PTD. With regard to the separation of U(VI) and Am(III), Am(III) is best extracted at a moderate concentration of HNO_3, with a maximum $SF_{Am/U}$ of 41.23.

Table 5: Separation factors $SF_{Am/M}$ (M=Eu, Cm, Pu, U) for extractions with 0.2 mol/L Me-TDDGA in n-dodecane and 0.02 mol/L PTD in different HNO_3 concentrations, including 10^{-5} mol/L Ln(III) (without Pm and Y) and ^{41}Am, ^{244}Cm, ^{152}Eu, ^{239}Pu, ^{237}Np, U-nat, T = 22°C ± 1°C, mixing time t=30 min.

	c(Me-TDDGA)=0.2 mol/L, c(PTD)=0.02 mol/L			
c(HNO_3) [mol/L]	**$SF_{Eu/Am}$**	**$SF_{Cm/Am}$**	**$SF_{Am/Pu}$**	**$SF_{Am/U}$**
0.052	-	-	-	-
0.237	8.78	-	-	-
0.58	10.14	1.10	0.25	0.35
1.074	6.78	1.51	0.88	4.10
2.009	-	0.23	6.00	41.23
3.38	-	0.13	9.00	27.40

In terms of the extraction behavior of the lanthanides in the presence of Me-TDDGA and PTD while varying the HNO_3 concentration, Figure 26 shows the distribution ratio of the different elements as a function of HNO_3 concentration. For each element, the D values increase continuously with increasing HNO_3 concentration, with the maximum D value being reached at the highest HNO_3 concentration. Within the series elements and at moderate HNO_3 concentration, the D values increase gradually until they reach a maximum at Er(III), as can be seen in Figure 27) This behaviour is similar to Me-TDDGA alone. At higher HNO_3 concentrations (c=2.0 and 3.4 mol/L), the D values increase, and Lu reaches the maximum D value. Y(III) behaves like a heavy lanthanide and has D values that lie between Tb(III) and Ho(III). At c(HNO_3)=1.1 mol/L, $D_{Am(III)}$=1.2 and $D_{Cm(III)}$=1.6, the values above 1 are in the range of $D_{Ln(III)}$ values between Nd(III) and Sm(III), here it becomes clear that a selective separation of An(III) from Ln(III) is not possible.

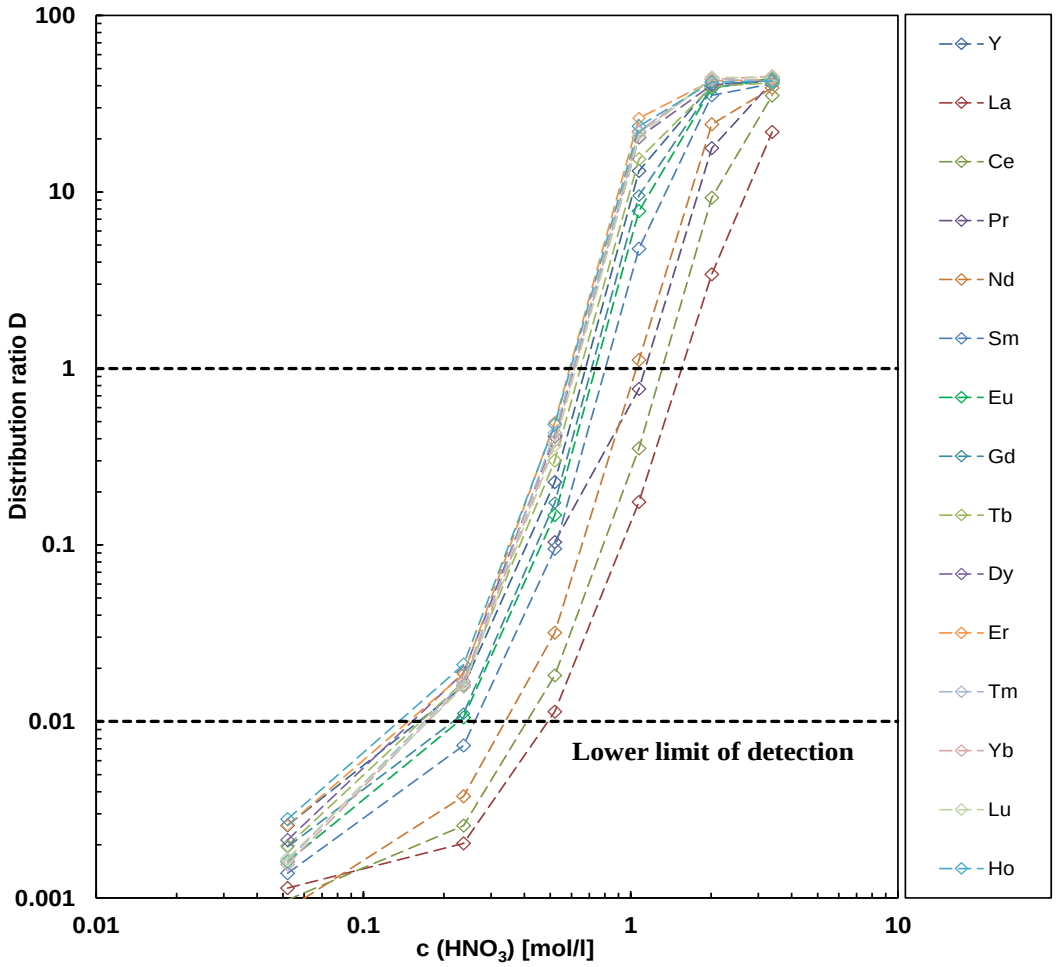

Figure 26: Distribution ratios of Ln(III) (without Pm,+Y) as a function of HNO_3 concentration for extraction with 0.2 mol/L Me-TDDGA in n-dodecane and 0.02 mol/L PTD.

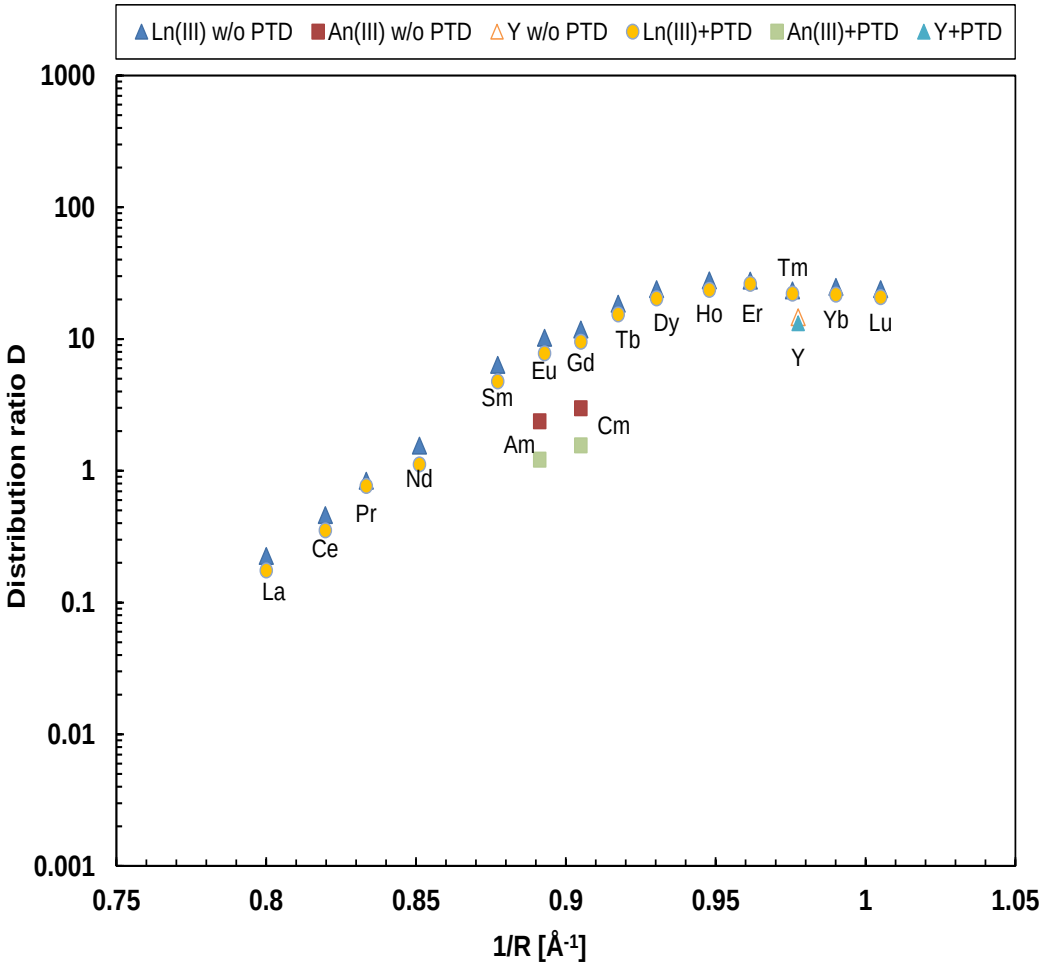

Figure 27: Distribution ratios of Am(III), Cm(III) and Ln(III) (without Pm, +Y,) as a function of the inverse radius with 0.2 mol/L Me-TDDGA in n-dodecane, in the presence and the absence of PTD (0.02 mol/L) in 1.074 mol/L HNO_3.

5 Conclusions and Outlook

In this work, a newly emerging ligand belonging to the DGA family was investigated for its ability to extract trivalent actinides and lanthanides. Me-TDDGA was classically dissolved in *n*-dodecane in the organic phase and contacted with an aqueous phase consisting of nitric acid and radiotracers for batch extraction experiments. Extraction with Me-TDDGA was found to be rapid under the extraction conditions tested (T=22°C, mixing time t = 30 min), with equilibrium being reached within the first 10 minutes. Both nitric acid and ligand concentrations were varied and, in agreement with the law of mass action, an increase in nitric acid concentration and ligand concentration was accompanied by an increase in the distribution ratios of all metal ions present. An interesting trend was observed among the lanthanides, where the maximum value of the partition ratio is reached at Er(III) before decreasing for the remaining heavy elements. A slope analysis was also performed to determine the complexation behavior. Predictably and typically for diglycolamides, 3:1 and 4:1 complexes with trivalent actinides and lanthanides were observed. Furthermore, the temperature variation experiment revealed the exothermic nature of the extraction with Me-TDDGA. With increasing temperature, the distribution ratios of the metal elements decrease significantly. However, an anomalous trend was observed for Pu(IV) and U(VI), where the D values increased at a higher temperature, precisely at T = 35°C. This could be due to the formation of different extracted species of the considered metals at different temperatures.

Then the formation of the third phase of nitric acid and Nd(III) as well as Th(IV) in Me-TDDGA dissolved in *n*-dodecane was evaluated. The distribution ratios and the concentrations of Nd(III) and Th(IV) in the organic phase were plotted against their initial concentrations in the aqueous phase. For Nd(III), $[Nd^{3+}]_{org}$. reached a maximum at a value of about 0.068 mol/L, after which it dropped sharply, indicating the formation of the third phase. The maximum loading capacity of 0.2 mol/L Me-TDDGA should be about 0.067 mol/L, which corresponds to the experimentally determined value. With respect to Th(IV), a thick and highly viscous phase was formed as the third phase, and the distribution ratios appear to be stable despite the increase in Th concentrations in the samples, instead of steadily increasing before dropping off when the organic phase was split off. The high susceptibility of DGA forming of a third phase in an *n*-dodecane/nitric acid system is well documented in the literature, especially with TODGA. In the case of Me-TDDGA, the introduction of a phase modifier would ideally suppress the third phase or at least improve the loading of metals. A further investigation of this is required.

The last part was dedicated to the testing of combined extraction systems to enable the separation of actinides from lanthanides. This was achieved by introducing two hydrophilic co-extractants: SO_3-Ph-BTP and PTD in different nitric acid concentrations. With SO_3-Ph-BTP, a high $SF_{Eu/Am}$ value of about 200 to 300 was achieved, indicating a high selectivity for Am(III) over Eu(III). Surprisingly, and in contrast to the results in the literature, no large $SF_{Eu/Am}$ values were obtained with PTD, so no meaningful separation of Am and Eu was observed. For both co-extractants, a decrease in separability with increasing HNO_3 concentration is also observed,

which is attributed to the increase in the degree of protonation of the ligand and thus to the decrease in the concentration of the free ligand.

Me-TDDGA alone is not able to separate An(III) from Ln(III). However, the introduction of a co-extractant led to promising results. Optimization of the experimental conditions is required, especially with regard to PTD, where an increase in concentration could have a positive influence on the SF values. Further investigations could be carried out regarding the radiolytic stability of the ligand and the determination of possible degradation products. In addition, a detailed speciation analysis of the metal-ligand complexes, possibly using spectroscopic techniques such as UV-Vis, NMR or EXAFS, would provide valuable insights into the coordination environment and extraction mechanisms. Furthermore, the influence of metal oxidation states, especially for Pu(IV) and Np(V), should be more thoroughly investigated, given the significant impact these states have on extraction behaviour. This would enable the construction of a robust extraction system capable of separating lanthanides and actinides from spent nuclear fuel.

Overall, these findings could be a step towards refining ligand design and separation strategies and bring us closer to more efficient and sustainable solutions for the separation of actinides and lanthanides.

6 References

1. IAEA, *NUCLEAR POWER AND SUSTAINABLE DEVELOPMENT*. 2016.
2. International Atomic Energy Agency (IAEA), *Nuclear Energy for a Net Zero World*. 2021: Vienna, Austria.
3. Modolo, G., A. Geist, and M. Miguirditchian, *Minor actinide separations in the reprocessing of spent nuclear fuels: recent advances in Europe*, in *Reprocessing and Recycling of Spent Nuclear Fuel*, R. Taylor, Editor. 2015, Woodhead Publishing: Oxford. p. 245-287.
4. Hill, C., *Overview of Recent Advances in An(III)/Ln(III) Separation by Solvent Extraction*, in *Ion Exchange and Solvent Extraction, A Series of Advances*, B.A. Moyer, Editor. 2009, CRC Taylor and Francis. p. 119-193.
5. Lanham, W.B. and T.C. Runion, *PUREX Process for Plutonium and Uranium Recovery*. 1949, Oak Ridge National Laboratory: Oak Ridge, TN, USA.
6. Veliscek-Carolan, J., *Separation of Actinides from Spent Nuclear Fuel: A Review.* J. Hazard. Mater., 2016. **318**: p. 266-281.
7. Hudson, M.J., F.W. Lewis, and L.M. Harwood, *The Circuitous Journey from Malonamides to BTPhens: Ligands for Separating Actinides from Lanthanides*, in *Strategies and Tactics in Organic Synthesis*, H. Michael, Editor. 2013, Academic Press: London. p. 177-202.
8. Bünzli, J.-C., *Lanthanides*. 2013. p. 1-43.
9. Beauvy, M., et al., *Treatment and recycling of spent nuclear fuel: Actinide partitioning – Application to waste management*. DEN Monographs, A Nuclear Energy Division Monograph, CEA. 2008, CEA, 91191 Gif-sur-Yvette Cedex, France: Pradel, Philippe.
10. Pearson, R.G., *The HSAB Principle — more quantitative aspects.* Inorg. Chim. Acta, 1995. **240**(1–2): p. 93-98.
11. Pearson, R.G., *Hard and soft acids and bases—the evolution of a chemical concept.* Coord. Chem. Rev., 1990. **100**: p. 403-425.
12. Choppin, G.R., *Comparison of the solution chemistry of the actinides and lanthanides.* Journal of the Less Common Metals, 1983. **93**(2): p. 323-330.
13. D'Angelo, P., et al., *Hydration Properties and Ionic Radii of Actinide(III) Ions in Aqueous Solution.* Inorg. Chem., 2013. **52**(18): p. 10318-10324.
14. D'Angelo, P., et al., *Revised Ionic Radii of Lanthanoid(III) Ions in Aqueous Solution.* Inorg. Chem., 2011. **50**(10): p. 4572-4579.
15. Madic, C. and M.J. Hudson, *High-Level Liquid Waste Partitioning by Means of Completely Incinerable Extractants*. 1998, European Commission: Luxembourg.
16. Vu, T.H., et al., *Liquid/Liquid Extraction Kinetics of Eu(III) and Am(III) by Extractants Designed for the Industrial Reprocessing of Nuclear Wastes.* Ind. Eng. Chem. Res., 2020. **59**(30): p. 13477-13490.
17. International Atomic Energy Agency (IAEA), *Assessment of Partitioning Processes for Transmutation of Actinides*. 2010: Vienna.
18. Geist, A., et al., *An Overview of Solvent Extraction Processes Developed in Europe for Advanced Nuclear Fuel Recycling, Part 1 - Heterogeneous Recycling.* Sep. Sci. Technol., 2021. **56**(11): p. 1866-1881.
19. Serrano-Purroy, D., et al., *Recovery of minor actinides from HLLW using the DIAMEX process.* Radiochim. Acta, 2005. **93**(6): p. 351-355.
20. Geist, A., et al., *6,6'-Bis(5,5,8,8-tetramethyl-5,6,7,8-tetrahydro-benzo[1,2,4]triazin-3-yl)[2,2']bipyridine, an effective extracting agent for the separation of americium(III) and curium(III) from the lanthanides.* Solvent Extr. Ion Exch., 2006. **24**(4): p. 463-483.

21. Lewis, F.W., et al., *Highly Efficient Separation of Actinides from Lanthanides by a Phenanthroline-Derived Bis-triazine Ligand.* J. Am. Chem. Soc., 2011. **133**(33): p. 13093-13102.
22. Lewis, F.W., et al., *BTBPs versus BTPhens: Some Reasons for Their Differences in Properties Concerning the Partitioning of Minor Actinides and the Advantages of BTPhens.* Inorg. Chem., 2013. **52**(9): p. 4993-5005.
23. Trumm, S., et al., *An Improved Hydrolytically-Stable Bis-Triazinyl-Pyridine (BTP) for Selective Actinide Extraction.* Solvent Extr. Ion Exch., 2011. **29**(2): p. 213-229.
24. Geist, A., et al. *Minor Actinide Separation: Simplification of the DIAMEX-SANEX Strategy by Means of Novel SANEX Processes*. in *GLOBAL 2013 "Nuclear Energy at a Crossroad"*. 2013. Salt Lake City, UT, USA.
25. Modolo, G., et al., *Development and demonstration of innovative partitioning processes (i-SANEX and 1-cycle SANEX) for actinide partitioning.* Progr. Nucl. Energ., 2014. **72**: p. 107-114.
26. Wilden, A., et al., *Selective actinide(III) separation using 2,6-bis[1-(propan-1-ol)-1,2,3-triazol-4-yl]pyridine (PyTri-Diol) in the innovative-SANEX process: laboratory scale counter current centrifugal contactor demonstration.* Radiochim. Acta, 2022. **110**(6-9): p. 515-525.
27. Clark, A., P. Yang, and J. Shafer, *Coordination of Actinides and the Chemistry Behind Solvent Extraction*. 2018.
28. Wilden, A., et al., *Direct Selective Extraction of Actinides (III) from PUREX Raffinate using a Mixture of CyMe$_4$BTBP and TODGA as 1-cycle SANEX Solvent.* Solvent Extr. Ion Exch., 2011. **29**(2): p. 190-212.
29. Ansari, S.A., et al., *Chemistry of Diglycolamides: Promising Extractants for Actinide Partitioning.* Chem. Rev., 2012. **112**(3): p. 1751-1772.
30. Fialová, K.O., et al., *Novel simplified synthesis of diglycolamides extractants.* J. Radioanal. Nucl. Chem., 2023: p. 8.
31. Nomizu, D., et al., *Complex formation of light and heavy lanthanides with DGA and DOODA, and its application to mutual separation in DGA-DOODA extraction system.* J. Radioanal. Nucl. Chem., 2022. **DOI:10.1007/s10967-022-08204-5**.
32. Sasaki, Y., et al., *The Novel Extractants, Diglycolamides, for the Extraction of Lanthanides and Actinides in HNO$_3$-n-dodecane System.* Solvent Extr. Ion Exch., 2001. **19**(1): p. 91-103.
33. Sasaki, Y., et al., *Complexation and back extraction of various metals by water-soluble diglycolamide.* Anal. Sci., 2007. **23**(6): p. 727-731.
34. Sasaki, Y., et al., *New water-soluble organic ligands for actinide cations complexation.* Chem. Lett., 2006. **35**(3): p. 256-257.
35. Whittaker, D., et al., *Applications of Diglycolamide Based Solvent Extraction Processes in Spent Nuclear Fuel Reprocessing, Part 1: TODGA.* Solvent Extr. Ion Exch., 2018. **36**(3): p. 223-256.
36. Tachimori, S., Y. Sasaki, and S. Suzuki, *Modification of TODGA-n-dodecane solvent with a monoamide for high loading of lanthanides(III) and actinides(III).* Solvent Extr. Ion Exch., 2002. **20**(6): p. 687-699.
37. Modolo, G., et al., *Development of a TODGA based Process for Partitioning of Actinides from a PUREX Raffinate Part I: Batch Extraction Optimization Studies and Stability Tests.* Solvent Extr. Ion Exch., 2007. **25**(6): p. 703-721.
38. Sasaki, Y., et al., *A method for the determination of extraction capacity and its application to N,N,N',N'-tetraalkylderivatives of diglycolamide-monoamide/n-dodecane media.* Anal. Chim. Acta, 2005. **543**(1-2): p. 31-37.

39. Malmbeck, R., D. Magnusson, and A. Geist, *Modified Diglycolamides for Grouped Actinide Separation.* J. Radioanal. Nucl. Chem., 2017. **314**(3): p. 2531-2538.
40. Verlinden, B., et al., *Solvent Optimization Studies for a New EURO-GANEX Process with 2,2'-Oxybis(N,N-di-n-decylpropanamide) (mTDDGA) and its Radiolysis Products.* Solvent Extr. Ion Exch., 2023. **41**(1): p. 59-87.
41. Wilden, A., et al., *Modified Diglycolamides for the An(III) + Ln(III) Co-separation: Evaluation by Solvent Extraction and Time-Resolved Laser Fluorescence Spectroscopy.* Solvent Extr. Ion Exch., 2014. **32**(2): p. 119-137.
42. Sharov, V.E. and G.V. Kostikova, *Specific features of temperature influence on the extraction of Am(III), Eu(III) and Lu(III) by N,N,N',N'-tetraoctyldiglycolamide from mineral acid solutions.* J. Radioanal. Nucl. Chem., 2024. **DOI:10.1007/s10967-024-09902-y**.
43. Hu, X.Y., et al., *Diglycolamide with long C-chains combined with ether bonds for high loading of Am(III) and Eu(III): Extraction, aggregation, and third-phase formation studies.* Sep. Purif. Technol., 2025. **360**(3): p. 131113.
44. Brown, J., et al., *Plutonium loading of prospective grouped actinide extraction (GANEX) solvent systems based on diglycolamide extractants.* Solvent Extr. Ion Exch., 2012. **30**(2): p. 127-141.
45. Bhattacharyya, A., et al., *Highly efficient separation of Am3+ and Eu3+ using an aqueous soluble sulfonated BTP derivative by hollow-fiber supported liquid membrane containing TODGA.* Sep. Sci. Technol., 2019. **54**(9): p. 1512-1520.
46. Geist, A., et al., *Actinide(III)/lanthanide(III) Separation Via Selective Aqueous Complexation of Actinides(III) Using a Hydrophilic 2,6-Bis(1,2,4-Triazin-3-yl)-Pyridine in Nitric Acid.* Solvent Extr. Ion Exch., 2012. **30**(5): p. 433-444.
47. Edwards, A.C., et al., *Hydrophilic 2,9-bis-triazolyl-1,10-phenanthroline ligands enable selective Am(III) separation: a step further towards sustainable nuclear energy.* Chem. Commun., 2017. **53**(36): p. 5001-5004.